ACCURATE TORQUE PULSATION ESTIMATION AND REDUCTION OF IPMSMS VALID FOR ANY OPERATING POINT AND CURRENT WAVEFORM

By

Tiraruek Ruekamnuaychok

A THESIS

Submitted to
Michigan State University
in partial fulfillment of the requirements
for the degree of

Electrical Engineering—Master of Science

2019

ABSTRACT

ACCURATE TORQUE PULSATION ESTIMATION AND REDUCTION OF IPMSMS VALID FOR ANY OPERATING POINT AND CURRENT WAVEFORM

By

Tiraruek Ruekamnuaychok

In this thesis, a method to estimate the torque pulsation of IPMSMs is proposed. The method is based on an analytical torque equation of IPMSMs derived by using the concepts of energy and co-energy of a magnetic circuit. This method is valid and accurate for any operating point, including that under heavy magnetic saturation, and for any arbitrary current waveform. Also, by using the proposed equation, a method to reduce the torque pulsation is proposed. Simulation and experimental results show that the proposed methods, for both estimation and reduction, are valid, accurate and effective.

ACKNOWLEDGMENTS

I would like to thank Prof. Elias G. Strangas, my advisor, for giving me knowledge and understanding regarding electrical machines and drives and all the support he made. Also, I would like to thank Shaopo Huang, a visiting scholar from Hebei University of Technology, for helping me in the experimental setup.

TABLE OF CONTENTS

LIST OF FIGURES

Chapter 1

Introduction

Interior Permanent Magnet Synchronous Motors (IPMSMs) are used widely nowadays due to many of their advantages such as high power density and high efficiency. Nevertheless, one of their main disadvantages is that they may have high torque pulsation.

The term "torque pulsation" refers to any oscillation that exists in the developed torque of a motor. This oscillation can lead to many negative effects such as audible noise and rotor speed variation. More importantly, it creates vibrations which can seriously damage a motor or any other thing connected to it.

For IPMSMs, the torque pulsation can have many components that are from many different sources such as control scheme, power converter and noise. However, its dominating component is usually from the construction of the motor itself. This work focuses solely on this component and assumes that all other components are zero. Note that throughout this work, whenever the term torque pulsation is used, it refers to this component.

Ideally, the construction of IPMSMs should be such that the stator winding and the radial magnetic flux density produced by the magnets are sinusoidally distributed in space. In this case, the developed torque will be constant as long as the phase current is purely sinusoidal. Unfortunately, such construction is not possible in practical situations. As a result, there will be the torque pulsation even if the phase current does not have harmonics.

Over the years, there have been many attempts in reducing the torque pulsation of IPMSMs. The most commonly used control method in doing so is called "Current Harmonic Injection." Its concept is to obtain the torque pulsation first. Then, inject current with some harmonics in order to have them compensate for the pulsation. In this case, the difficulty lies mainly in how the torque pulsation itself is obtained.

Generally, there are two ways to obtain it. The first way is to use a torque transducer. However, its installation is not convenient, and it is likely to have some error. Moreover, what it actually measures is not the developed torque of a motor. Rather, it measures the shaft torque which is the developed torque passed through the transfer function of the shaft. Therefore, injecting current harmonics based on this torque may not be as effective as desired.

The other way is to obtain by estimation. In literature, there have been many attempts in deriving an analytical torque equation of IPMSMs that takes the torque pulsation into consideration [3–17]. Some of them derived the torque equation by using the product of back-emfs and currents [2–5]. Some of them analyzed harmonics contained in the general torque equation [6–8]. Alternatively, [9, 10] derived the torque equation with focus on derivative of inductances with respect to the rotor position. However, these works usually considered only some components of the torque pulsation, not the total one.

In recent years, the trend in deriving the analytical torque equation is based on the concepts of energy and co-energy of a magnetic circuit [11–17]. In [13], N. Nakao and K. Akatsu proposed an analytical equation for the torque of IPMSMs, including the torque pulsation, based on the concept of co-energy. Nevertheless, the co-energy in this work was not thoroughly defined, and the structure of the equation itself was based on an assumption that the magnetic saturation was linear.

In short, until now, there has been no analytical torque equation of IPMSMs that takes all components of the torque pulsation into consideration, is complete in derivation and is valid for any operating point, including that under heavy magnetic saturation. This work proposes such an equation together with offline algorithms that make use of it. Then, based on the proposed equation, a method to reduce the torque pulsation based on the current harmonic injection is developed. Simulation and experimental results show that the equation, algorithms and reduction method, are valid, accurate and effective.

Chapter 2

Calculation of Stored Field Energy, Stored Field Co-Energy and Torque of a Magnetic Circuit

The calculation of the stored field energy, stored field co-energy and torque of a magnetic circuit are very important in this work. They serve as fundamental in deriving the total torque equation of IPMSMs. In this chapter, they will be reviewed in detail.

2.1 Calculation of Stored Field Energy

For a magnetic circuit, the term "stored field energy" refers to the energy that is stored inside the circuit in the form of magnetic field. Neglecting losses, it can be identified by taking difference between the input and output energy.

Consider a magnetic circuit with one electrical input and one mechanical output in Fig. 2.1 where e is induced voltage, i is injected current, ϕ is magnetic flux, λ is total magnetic flux linkage and θ is the angle of rotation. The electrical input power, P_e, is given by (2.1). The total input energy from initial time t_0 to final time t_f, denoted by $\Delta W^e_{t_0 \to t_f}$, can be calculated by integrating the electrical input power over the time period as (2.2).

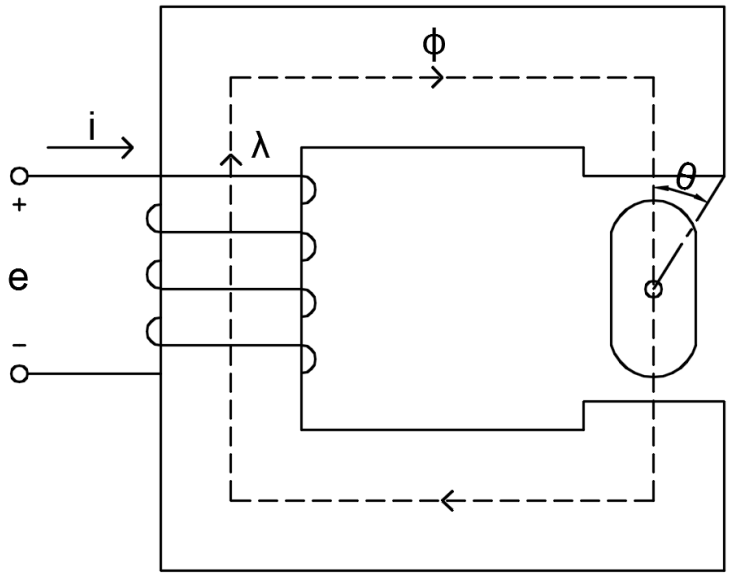

Figure 2.1: Magnetic circuit with one electrical input and one mechanical output.

$$\begin{aligned} P_e &= ie \\ &= i\frac{d\lambda}{dt} \end{aligned} \tag{2.1}$$

$$\begin{aligned} \Delta W^e_{t_0 \to t_f} &= \int_{t_0}^{t_f} P_e dt \\ &= \int_{t_0}^{t_f} i\frac{d\lambda}{dt} dt \\ &= \int_{\lambda_0}^{\lambda_f} i d\lambda \end{aligned} \tag{2.2}$$

The output mechanical power, denoted by P_m, can be calculated as (2.3) where T is electromagnetic torque in Nm. Consequently, the total output energy from initial time t_0 to final time t_f, denoted by $\Delta W^m_{t_0 \to t_f}$, can be calculated by integrating the mechanical output power over the time period as (2.4).

$$P_m = T\frac{d\theta}{dt} \tag{2.3}$$

$$\begin{aligned} \Delta W^m_{t_0 \to t_f} &= \int_{t_0}^{t_f} P_m dt \\ &= \int_{t_0}^{t_f} T\frac{d\theta}{dt} dt \\ &= \int_{\theta_0}^{\theta_f} T d\theta \end{aligned} \tag{2.4}$$

By taking the difference between the input and output energy, the stored field energy from initial time t_0 to final time t_f, denoted by $\Delta W^f_{t_0 \to t_f}$ can be expressed as (2.5).

$$\begin{aligned} \Delta W^f_{t_0 \to t_f} &= \Delta W^e_{t_0 \to t_f} - \Delta W^m_{t_0 \to t_f} \\ &= \int_{\lambda_0}^{\lambda_f} i d\lambda - \int_{\theta_0}^{\theta_f} T d\theta \end{aligned} \tag{2.5}$$

Note that (2.5) can be interpreted as a line integral scalar function defined on a 2-dimensional space (λ, θ), and its alternative meaning is the difference of the stored field energy between the initial state (λ_0, θ_0) and the final state (λ_f, θ_f).

Taking the initial state to be $(\lambda_0 = 0, \theta_0 = 0)$ the stored field energy at the final state (λ_f, θ_f), denoted by W_f^f, can be calculated by (2.6).

$$W_f^f = \int_0^{\lambda_f} id\lambda - \int_0^{\theta_f} Td\theta \tag{2.6}$$

By neglecting the hysteresis loss, the stored field energy becomes conversative and the path of integration from the initial state $(0, 0)$ to the final state (λ_f, θ_f) in (2.6) can be arbitrarily chosen. The simplest path is to integrate along the direction of θ from $\theta = 0$ to $\theta = \theta_f$ first while keeping λ fixed at zero, i.e., to integrate from $(0, 0)$ to $(0, \theta_f)$. In this integration, (2.6) is zero. This is because when λ is kept zero, $d\lambda$ will also be zero. Moreover, there will be no magnetization which results in zero T. After that, integrate from $(0, \theta_f)$ to (λ_f, θ_f). Using this integration path, the stored field energy at any final state (λ_f, θ_f) can be calculated as (2.7) where the vertical line represents the fact that θ is kept fixed at θ_f. Fig. 2.2 illustrates this calculation. Note that to use (2.7), the function $i(\lambda, \theta)$ must be known. Theoretically, if the exact geometry of the magnetic circuit is known, the function can be analytically obtained. In Fig. 2.2, the blue dot line represents this function at θ_f.

$$W_f^f = \int_0^{\lambda_f} id\lambda \Big|_{\theta_f} \tag{2.7}$$

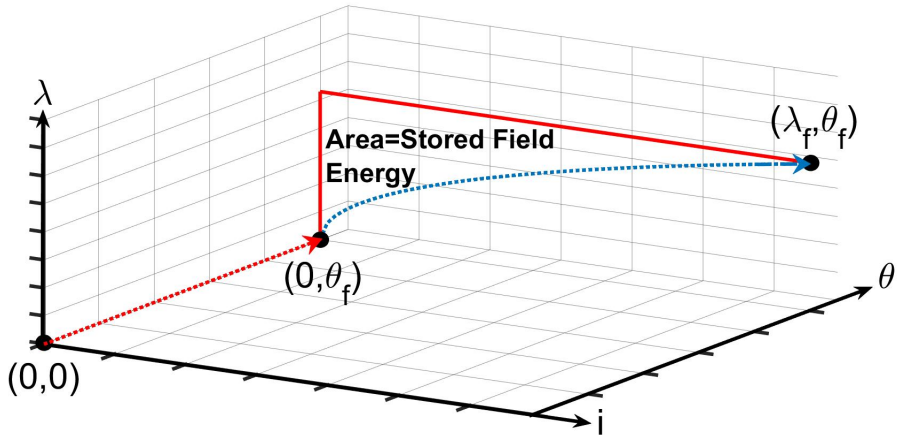

Figure 2.2: Integration path for the calculation of the stored field energy at any final state (λ_f, θ_f).

2.2 Calculation of Torque from Stored Field Energy

By using the fact that the stored field energy (2.6) is a function of two variables, which are λ and θ, the differential of the stored field energy can be expressed as (2.8).

$$dW^f = \frac{\partial W^f}{\partial \lambda} d\lambda + \frac{\partial W^f}{\partial \theta} d\theta \tag{2.8}$$

Moreover, according to (2.5) and (2.6), the differential of the stored field energy can also be expressed as (2.9).

$$dW^f = i d\lambda - T d\theta \tag{2.9}$$

By comparing the last terms of (2.8) and (2.9), the torque of the magnetic circuit can be expressed as (2.10).

$$T = -\frac{\partial W^f}{\partial \theta} \tag{2.10}$$

2.3 Calculation of Stored Field Co-Energy

Calculating the torque from the stored field energy is somewhat inconvenient. This is due to the fact that it requires integration of the current with respect to the flux linkage, which is not intuitive. A more convenient way of calculating the torque is to calculate through the "stored field co-energy." Note that the stored field co-energy is not a physical quantity. Rather, it is a concept that is defined and developed just to simplify the calculation.

In this section, calculation of the stored field co-energy for the given magnetic circuit will be presented. Then, in the following section, calculation of the torque by using this co-energy concept will be discussed.

For the magnetic circuit shown in Fig. 2.1 with the stored field energy equation of (2.6), the stored field co-energy at the state (λ_f, θ_f), denoted by W_f^c is defined as (2.11).

$$W_f^c = i_f \lambda_f - W_f^f \tag{2.11}$$

By substituting the stored field energy (2.6) into (2.11), it yields

$$W_f^c = i_f \lambda_f - \int_0^{\lambda_f} i d\lambda + \int_0^{\theta_f} T d\theta \tag{2.12}$$

Note that

$$i_f \lambda_f - \int_0^{\lambda_f} i d\lambda = \int_0^{i_f} \lambda di$$

Hence, (2.12) is changed to (2.13), with the 2-dimensional space of (i, θ).

$$W_f^c = \int_0^{i_f} \lambda di + \int_0^{\theta_f} T d\theta \tag{2.13}$$

Similar to the stored field energy, (2.13) is conservative under the assumption that the hysteresis loss is neglected. Following the same path of integration but with respect to i, the stored field co-energy at the final state (λ_f, θ_f) is given by (2.14). For virtualization, see Fig. 2.3.

$$W_f^c = \int_0^{i_f} \lambda di \Big|_{\theta_f} \tag{2.14}$$

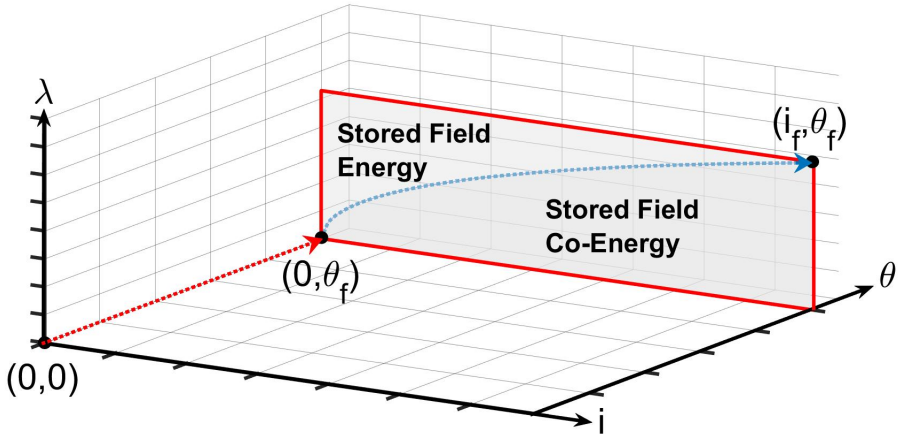

Figure 2.3: Integration path for the calculation of the stored field co-energy at any final state (i_f, θ_f).

2.4 Calculation of Torque from Stored Field Co-Energy

Following the same logic from the stored field energy, the differential of the stored field co-energy can be expressed as (2.15) and (2.16).

$$dW^c = \frac{\partial W^c}{\partial i} di + \frac{\partial W^c}{\partial \theta} d\theta \tag{2.15}$$

$$dW^c = \lambda di + T d\theta \tag{2.16}$$

By comparing each term of these two equations, the torque of the magnetic circuit can be expressed by (2.17).

$$T = \frac{\partial W^c}{\partial \theta} \tag{2.17}$$

It can be seen in this chapter that the torque of the given magnetic circuit can be expressed using either the stored field energy or the stored field co-energy. Moreover, as long as the function $i(\lambda, \theta)$, or equivalently $\lambda(i, \theta)$, is known, its stored field energy, stored field co-energy and torque can be calculated immediately.

Note that even though this chapter focuses only on the magnetic circuit with one electrical input and one mechanical output, the concept itself is generally true of any other magnetic circuits, and it will serve as fundamental in deriving the total torque equation of IPMSMs in the next chapter.

Chapter 3

The Complete Torque Equation of IPMSMs

In this chapter, the complete torque equation of IPMSMs is derived. The derivation is based on the following concept. When an IPMSM is considered under the rotor frame of reference, its energy can be considered as having two components. The first component is the energy that is not stored in the form of magnetic field. The second component, on the other hand, is the energy that is stored in the form of magnetic field. To derive the torque equation, these two components will be identified first. Then, their corresponding torques will be derived separately. Finally, adding the two torques gives the total torque of IPMSMs.

3.1 Energy Decomposition

For IPMSMs, the input power can be expressed as (3.1) where e_{abc} and i_{abc} are phase back-emfs and currents respectively. Consequently, transforming (3.1) into the rotor frame of reference yields (3.2) where e_{dq} and i_{dq} are d-q axis back-emfs and currents.

$$P_{in} = e_a i_a + e_b i_b + e_c i_c \tag{3.1}$$

$$= \frac{3}{2}\big(e_d i_d + e_q i_q\big) \tag{3.2}$$

Note that the d-q axis back-emfs e_{dq} can be expressed as (3.3) and (3.4) where ω_e is electrical speed in rad/s and λ_{dq} are d-q axis total flux linkages.

$$e_d = -\omega_e \lambda_q + \frac{d\lambda_d}{dt} \tag{3.3}$$

$$e_q = \omega_e \lambda_d + \frac{d\lambda_q}{dt} \tag{3.4}$$

By substituting (3.3) and (3.4) into (3.2), the final expression for the input power of IPMSMs can be obtained as (3.5).

$$P_{in} = \frac{3}{2}\omega_e \left(\lambda_d i_q - \lambda_q i_d \right) + \frac{3}{2}\left(i_d \frac{d\lambda_d}{dt} + i_q \frac{d\lambda_q}{dt} \right) \tag{3.5}$$

The output power of IPMSMs can be expressed as (3.6) where T is the electromagnetic torque in Nm and θ_m is the mechanical rotor position in radians.

$$P_{out} = T \frac{d\theta_m}{dt} \tag{3.6}$$

The amount of energy being stored in the form of magnetic field from initial time t_0 to final time t_f, denoted by $\Delta W^f_{t_0 \to t_f}$, can be identified by taking integral of the difference between the input and output power as (3.7).

$$\Delta W^f_{t_0 \to t_f} = \int_{t_0}^{t_f} P_{in} dt - \int_{t_0}^{t_f} P_{out} dt \tag{3.7}$$

By substituting (3.5) and (3.6) in (3.7), the equation becomes (3.8), where P is the number of pole pairs.

$$\Delta W^{f}_{0\to f} = \int_{\theta_{m0}}^{\theta_{mf}} \frac{3}{2} P\big(\lambda_d i_q - \lambda_q i_d\big) d\theta_m + \frac{3}{2} \int_{\lambda_{d0}}^{\lambda_{df}} i_d d\lambda_d + \frac{3}{2} \int_{\lambda_{q0}}^{\lambda_{qf}} i_q d\lambda_q - \int_{\theta_{m0}}^{\theta_{mf}} T d\theta_m \tag{3.8}$$

Note that (3.8) can be considered as a line integral scalar function defined on a 3-dimensional space $(\lambda_d, \lambda_q, \theta_m)$ and its alternative physical interpretation is the difference of the stored energy between the initial state $(\lambda_{d0}, \lambda_{q0}, \theta_{m0})$ and the final state $(\lambda_{df}, \lambda_{qf}, \theta_{mf})$. In terms of usage, (3.8) is to be applied on the path on which the state is moved. For example, consider Fig. 3.1. Suppose at some initial time, the state is at $(\lambda_{d0}, \lambda_{q0}, \theta_{m0})$ and at the next time instance, the state is moved along the blue line to the final state $(\lambda_{df}, \lambda_{qf}, \theta_{mf})$. Then, this blue line is the path on which (3.8) is to be applied.

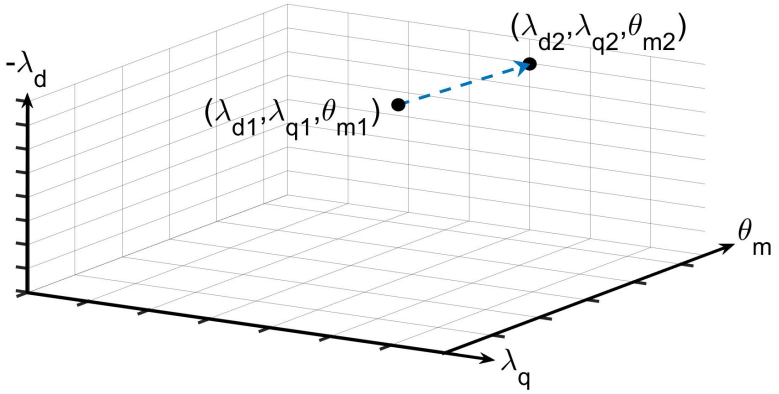

Figure 3.1: Some specific initial and final state of an IPMSM and its path.

However, by neglecting the hysteresis loss, the stored energy becomes conservative and hence, the integration path can be arbitrarily chosen. By taking the path as shown in Fig. 3.2, where the line $(\lambda_0, 0, \theta_m)$ represents any state that has zero i_{dq}, i.e., no current injected, it can be shown that the first term of (3.8) is always zero while the other terms are not. This concludes that for the given input power of (3.5), the input energy due to the first will not be stored in the form of magnetic field while the input energy due to the second term will.

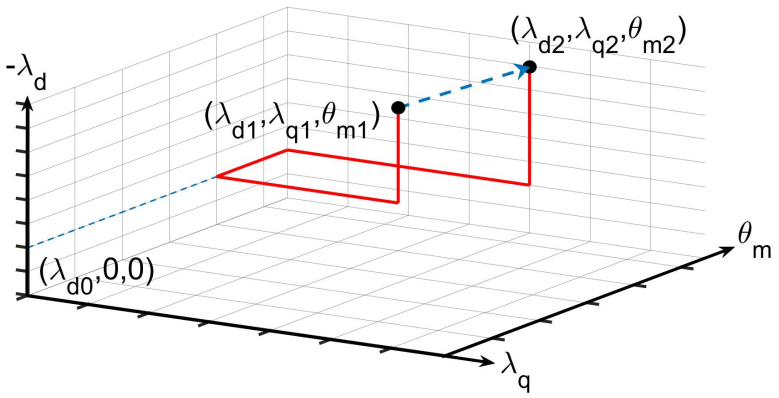

Figure 3.2: One possible integration path.

Following this logic, the energy of IPMSMs can be considered as having two components. The first component is called "instantaenous energy." It is the energy that is not stored in the form of magnetic field, and it corresponds to the input energy due to the first term of (3.5). The second component, on the other hand, is the energy that is stored in the form of magnetic field, and it corresponds to the input energy of the second term in (3.5) combined with the existing energy due to the magnets. In this work, this component is called "stored field energy."

3.2 Instantaneous Torque

Since the input energy due to the first term in (3.5), which is the first term in (3.8), is not stored in the form of magnetic field, it will be transferred directly to the output in the form of torque. This torque at any final state $(\lambda_{df}, \lambda_{qf}, \theta_{mf})$ can be derived by simply taking derivative of the energy itself with respect to the rotor position as (3.9) and will be called "instantaneous torque." Note that this torque is generally the main torque of the motor and it contains both constant and oscillating components.

$$T_{ins} = \frac{3}{2} P\big(\lambda_{df} i_{qf} - \lambda_{qf} i_{df}\big) \tag{3.9}$$

3.3 Stored Field Energy Torque

As mentioned earlier, in addition to the instantaneous energy, the motors also have the stored field energy, and the existence of this energy also develops torque. This torque is called in this work "stored field energy torque", and it can be derived as follows.

By removing the first term in (3.8), the amount of energy being stored in the form of magnetic field from any initial state to any final state can be expressed as (3.10).

$$\Delta W_{0\to f}^{f} = \frac{3}{2} \int_{\lambda_{d0}}^{\lambda_{df}} i_d d\lambda_d + \frac{3}{2} \int_{\lambda_{q0}}^{\lambda_{qf}} i_q d\lambda_q - \int_{\theta_{m0}}^{\theta_{mf}} T d\theta_m \tag{3.10}$$

By taking the initial state to be that when there is no i_{dq} with zero θ_m, i.e., $(\lambda_{d0}, 0, 0)$, with an assumption that at this state, the existing energy due to the magnets is K, the stored field energy of IPMSMs at any final state $(\lambda_{df}, \lambda_{qf}, \theta_{mf})$ can be expressed as (3.11).

$$W_f^f = \left[\frac{3}{2}\int_{\lambda_{d0}}^{\lambda_{df}} i_d d\lambda_d + \frac{3}{2}\int_0^{\lambda_{qf}} i_q d\lambda_q - \int_0^{\theta_{mf}} T d\theta_m\right] + K \tag{3.11}$$

By taking the differential of (3.11), the equation becomes (3.12).

$$dW_f^f = \frac{3}{2} i_d d\lambda_d + \frac{3}{2} i_q d\lambda_q - T d\theta_m \tag{3.12}$$

Furthermore, by using the fact that (3.11) is a function of three variables, its differential can also be expressed as (3.13).

$$dW_f^f = \frac{\partial W_f^f}{\partial \lambda_d} d\lambda_d + \frac{\partial W_f^f}{\partial \lambda_q} d\lambda_q + \frac{\partial W_f^f}{\partial \theta_m} d\theta_m \tag{3.13}$$

By comparing the terms of (3.12) and (3.13), the stored field energy torque can be expressed as (3.14).

$$T_{sfe} = -\frac{\partial W_f^f}{\partial \theta_m}. \tag{3.14}$$

Alternatively, dividing (3.12) by θ_m yields (3.15). Consequently, by rearranging (3.15), the stored field energy torque can also be expressed as (3.16).

$$\frac{dW_f^f}{d\theta_m} = \frac{3}{2} i_d \frac{d\lambda_d}{d\theta_m} + \frac{3}{2} i_q \frac{d\lambda_q}{d\theta_m} - T \tag{3.15}$$

$$T_{sfe} = \frac{3}{2} i_d \frac{d\lambda_d}{d\theta_m} + \frac{3}{2} i_q \frac{d\lambda_q}{d\theta_m} - \frac{dW_f^f}{d\theta_m} \tag{3.16}$$

As mentioned earlier, using the stored field energy is not convenient. In the following derivation, expression of the stored field energy torque in terms of the stored field co-energy will be presented.

For IPMSMs, the stored field co-energy at any final state $(\lambda_{df}, \lambda_{qf}, \theta_{mf})$ is defined as (3.17). Then, by substituting (3.11) into (3.17), the equation becomes (3.18). Note that the stored field co-energy is not a physical quantity. Rather, it is just a tool developed to simplify the calculation.

$$W_f^c = \frac{3}{2} i_{qf} \lambda_{qf} + \frac{3}{2} i_{df} \lambda_{df} - W_f^f \tag{3.17}$$

$$= \left[\frac{3}{2} i_{qf} \lambda_{qf} + \frac{3}{2} i_{df} \lambda_{df} - \frac{3}{2} \int_{\lambda_{d0}}^{\lambda_{df}} i_d d\lambda_d - \frac{3}{2} \int_0^{\lambda_{qf}} i_q d\lambda_q + \int_0^{\theta_{mf}} T d\theta_m \right] - K \tag{3.18}$$

In general, the relations between λ_d and i_d and between λ_q and i_q can be expressed as (3.19) and (3.20). For virtualization, see Fig. 3.3 and 3.4.

$$i_{df} \lambda_{df} = \int_{\lambda_{d0}}^{\lambda_{df}} i_d d\lambda_d + \int_0^{i_{df}} \lambda_d di_d \tag{3.19}$$

$$i_{qf} \lambda_{qf} = \int_0^{\lambda_{qf}} i_q d\lambda_q + \int_0^{i_{qf}} \lambda_q di_q \tag{3.20}$$

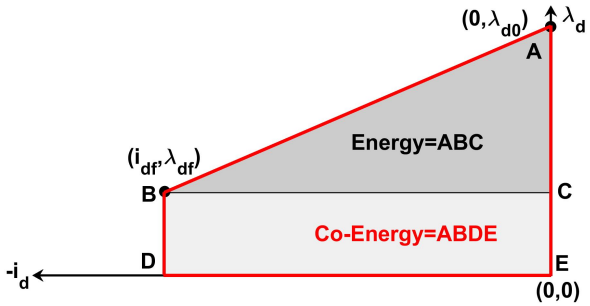

Figure 3.3: Relation between λ_d and i_d.

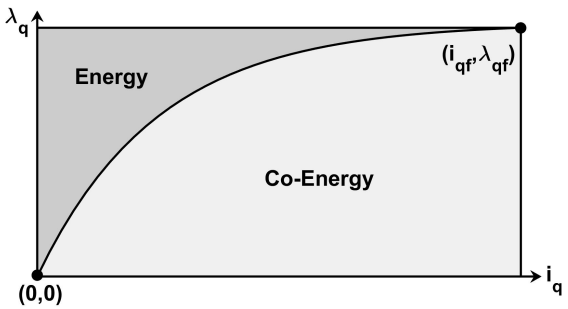

Figure 3.4: Relation between λ_q and i_q.

By using (3.19) and (3.20), the stored field co-energy (3.18) is reduced to (3.21), where the second term is negative since the integration is applied on a positive function but in negative direction.

$$W_f^c = \left[\frac{3}{2}\int_0^{i_{qf}} \lambda_q di_q + \frac{3}{2}\int_0^{i_{df}} \lambda_d di_d + \int_0^{\theta_{mf}} T d\theta_m\right] - K \tag{3.21}$$

For convenience in applying (3.21), the limit of integration of the second term is reverted so that the integration becomes positive. As a result, (3.21) becomes (3.22), which is the final expression for the stored field co-energy of IPMSMs at any final state $(\lambda_{df}, \lambda_{qf}, \theta_{mf})$. Note that (3.22) is still a line integral scalar function, but it is now defined on a 3-dimensional space of (i_d, i_q, θ_m). Also, by neglecting hysteresis loss, the conservative property still remains.

$$W_f^c = \left[\frac{3}{2}\int_0^{i_{qf}} \lambda_q di_q - \frac{3}{2}\int_{i_{df}}^{0} \lambda_d di_d + \int_0^{\theta_{mf}} T d\theta_m\right] - K \tag{3.22}$$

Taking the differential of stored field co-energy yields (3.23). Note that the differential must be taken on the original expression (3.21), not the one modified for convenience (3.22).

$$dW_f^c = \frac{3}{2}\lambda_q di_q - d\left[-\frac{3}{2}\int_0^{i_{df}} \lambda_d di_d \right] + T d\theta_m$$
$$= \frac{3}{2}\lambda_q di_q + \frac{3}{2}\lambda_d di_d + T d\theta_m \tag{3.23}$$

In addition, since the stored field co-energy is a function of three variables, its differential can also be expressed as

$$dW_f^c = \frac{\partial W_f^c}{\partial i_q} di_q + \frac{\partial W_f^c}{\partial i_d} di_d + \frac{\partial W_f^c}{\partial \theta_m} d\theta_m \tag{3.24}$$

Similar to the stored field energy, by comparing the terms of (3.23) and (3.24), the torque can be expressed as (3.25)

$$T_{sfe} = \frac{\partial W_f^c}{\partial \theta_m} \tag{3.25}$$

Alternatively, dividing (3.23) by θ_m yields (3.26). Consequently, by rearranging (3.26), the torque can be expressed as (3.27).

$$\frac{dW_f^c}{d\theta_m} = \frac{3}{2}\lambda_q \frac{di_q}{d\theta_m} + \frac{3}{2}\lambda_d \frac{di_d}{d\theta_m} + T \tag{3.26}$$
$$T_{sfe} = \frac{dW_f^c}{d\theta_m} - \frac{3}{2}\lambda_q \frac{di_q}{d\theta_m} - \frac{3}{2}\lambda_d \frac{di_d}{d\theta_m} \tag{3.27}$$

Up to this point, it can be seen that the stored field energy torque can be expressed in terms of the stored field energy as (3.14) and (3.16) or in terms of the stored field co-energy as (3.25) and (3.27).

The easiest and most practical expression is the one in the stored field co-energy term with normal derivative (3.27). The reason is that this equation explicitly includes the oscillation in the currents, i.e., $\frac{di_d}{dt}$ and $\frac{di_q}{dt}$, while (3.25) does not. This makes it easier to use in practical situations since most of the time, i_{dq} are not constant due to the fact that the current controllers are not ideal. Note that after this point, the derivation of the torque expression will be based on (3.27) only.

By integrating (3.22) from $\theta_m = 0$ to $\theta_m = \theta_{mf}$ with i_{dq} kept fixed at zero, and then integrating from $(i_d, i_q) = (0, 0)$ to $(i_d, i_q) = (i_{df}, i_{qf})$ with θ_m kept fixed at θ_{mf}, the stored field co-energy at any final state $(i_{df}, i_{qf}, \theta_{mf})$ can be calculated as (3.28), where the vertical lines represent that the integrations are evaluated at θ_{mf}. Note that (3.28) now represents a numerical value, not a function.

$$W_f^c = \left[\frac{3}{2} \int_0^{i_{qf}} \lambda_q di_q \Big|_{\theta_{mf}} - \frac{3}{2} \int_{i_{df}}^{0} \lambda_d di_d \Big|_{\theta_{mf}} \right] + \int_0^{\theta_{mf}} T_{cogging} d\theta_m - K \tag{3.28}$$

By substituting (3.28) into (3.27) and using the relation $\theta_e = P\theta_m$, where θ_e is the electrical position, the stored field energy torque at any final state $(i_{df}, i_{qf}, \theta_{ef})$ can be expressed as (3.29), where $\widetilde{W}_{id}^c$ and $\widetilde{W}_{iq}^c$ are defined as (3.30) and (3.31). Note that even though in terms of derivation, (3.29) is the stored field energy torque at any final state $(i_{df}, i_{qf}, \theta_{mf})$, but since the expression holds true for any final state, the 3-dimensional space of $(i_{df}, i_{qf}, \theta_{mf})$ can be changed to $(i_{df}, i_{qf}, \theta_{ef})$ without loss of generality. Also note that, according to (3.29), the stored field energy torque is expressed in terms of the derivative, therefore, this torque will have only oscillating components.

$$T_{sfe} = \frac{3}{2}P\left[\frac{d}{d\theta_e}\left(\widetilde{W}^c_{i_{qf},\theta_{ef}} - \widetilde{W}^c_{i_{df},\theta_{ef}}\right) - \lambda_{qf}\frac{di_{qf}}{d\theta_e} - \lambda_{df}\frac{di_{df}}{d\theta_e}\right] + T_{cogging} \tag{3.29}$$

$$\widetilde{W}^c_{i_{df},\theta_{ef}} = \left(\int_{i_{df}}^{0} \lambda_d di_d\right)\Bigg|_{\theta_{ef}} \tag{3.30}$$

$$\widetilde{W}^c_{i_{qf},\theta_{ef}} = \left(\int_{0}^{i_{qf}} \lambda_q di_q\right)\Bigg|_{\theta_{ef}} \tag{3.31}$$

3.4 Total Torque

Finally, adding the instantaneous and stored field energy together, the final expression for the torque of IPMSMs at any final state $(i_{df}, i_{qf}, \theta_{ef})$ can be expressed as (3.32).

$$T_{total} = \frac{3}{2}P\big(\lambda_{df}i_{qf} - \lambda_{qf}i_{df}\big) + \frac{3}{2}P\left[\frac{d}{d\theta_e}\left(\widetilde{W}^c_{i_{qf},\theta_{ef}} - \widetilde{W}^c_{i_{df},\theta_{ef}}\right) - \lambda_{qf}\frac{di_{qf}}{d\theta_e} - \lambda_{df}\frac{di_{df}}{d\theta_e}\right] + T_{cogging} \tag{3.32}$$

Chapter 4

Torque Pulsation Estimation Algorithm

It can be seen that to use the final equation (3.32), the relation between i_{dq}, λ_{dq} and θ_e must be known. Unfortunately, it is almost impossible to obtain the relation analytically due to many reasons such as the complexity of magnetic field calculation. Moreover, the equation itself is not straightforward; it requires the calculation of the stored field co-energy. Hence, in this chapter, an algorithm to identify the relation experimentally and consequently calculate the torque is proposed. Note that this algorithm contains an offline motor characterization which requires a motor to be connected to a dynamometer or a variable mechanical load.

In this entire work, the cogging torque $T_{cogging}$ is assumed to be known. In addition, to use (3.32), the exact waveforms of λ_{dq} are required. In this section, they are assumed to be known first. In a later section, a method of how to obtain them will be presented.

For simplicity, let the algorithm be explained along with an example. The motor used in the example is a 10-pole IPMSM with concentrated winding and fractional slot per pole per phase. Its rated current is 25A and the operating point is chosen at $i_d = -4$ and $i_q = 20$. Its 2-D cross section for FEA is shown in Fig. 4.1. Note that although the operating point in this example is assumed to be constant, the algorithm is actually valid for any arbitrary waveforms of i_{dq}.

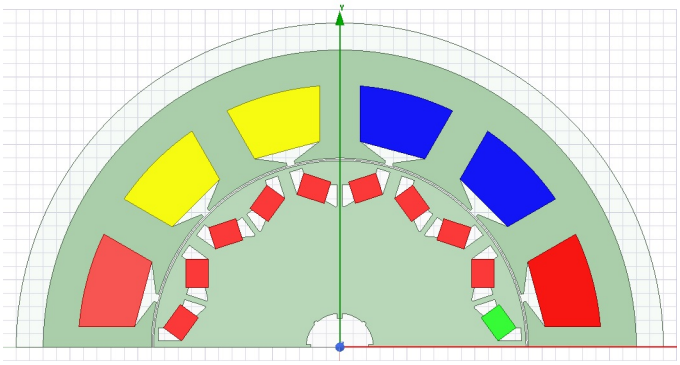

Figure 4.1: 2-D cross section for FEA.

4.1 Stored Field Energy Torque

In the algorithm, the stored field energy torque will be calculated first followed by the calculation of the instantaneous torque. Adding these two torques together gives the total torque of IPMSMs.

The following steps explain in detail of how to apply (3.29) to calculate the stored field energy torque for a given operating point over a range of electrical position.

1. Suppose that the given operating point is at (i_{dop}, i_{qop}). First, rotate the motor at some arbitrary rotor speed. Then, inject i_{dq} step by step from the origin $(0, 0)$ to the operating point. During the injection, the rotor speed is to be maintained. This is why a dynamometer or a variable mechanical load is required. The path for the injection can be arbitrarily chosen as long as the current at each step is increasing. Fig. 4.2 shows some possible paths of injection. The path can be from the origin to point a or b and then to the operating point. Alternatively, it can be directly from the origin to the operating point as the curve or the straight line. Then, at each step, collect i_{dq} and λ_{dq} for at least one electrical cycle. Note that at the origin, λ_{dq} are the flux linkages due to the magnets. Also note that after collecting the data at the operating point, the dynamometer or the variable mechanical load is no longer needed. As for the example,

the desired operating point is given as $i_d = -4, i_q = 20$. The injection path is chosen as $(i_d, i_q) = (-0.5, 2.5), (-1, 5), (-1.5, 7.5), (-2, 10), (-2.5, 12.5), (-3, 15), (-3.5, 17.5)$ and $(-4, 20)$.

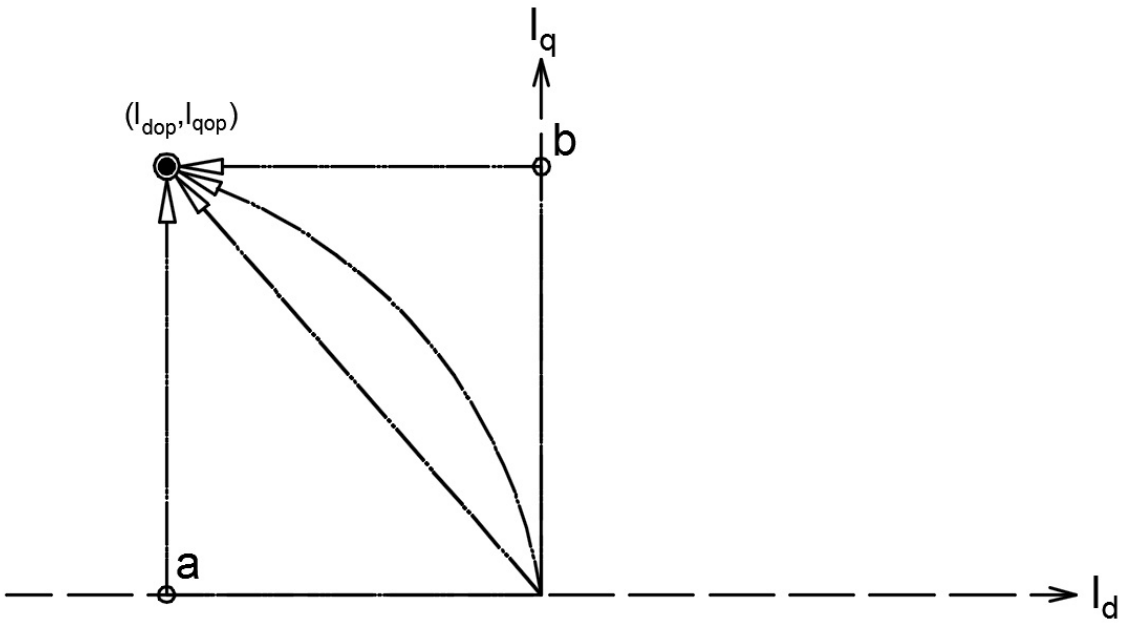

Figure 4.2: Operating point and some possible paths of injection.

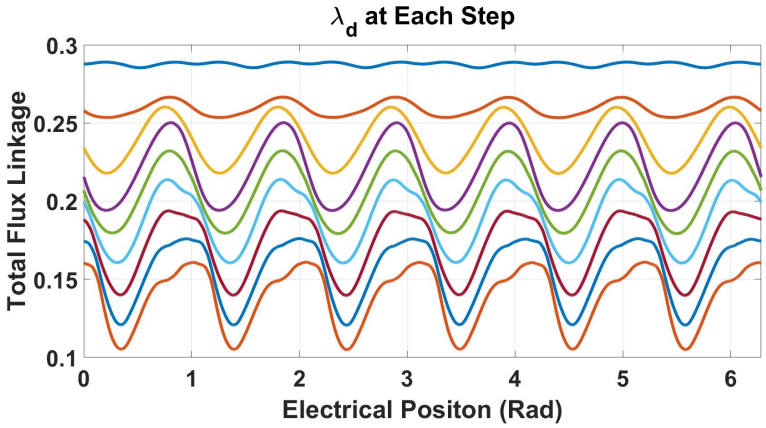

Figure 4.3: λ_d at each step.

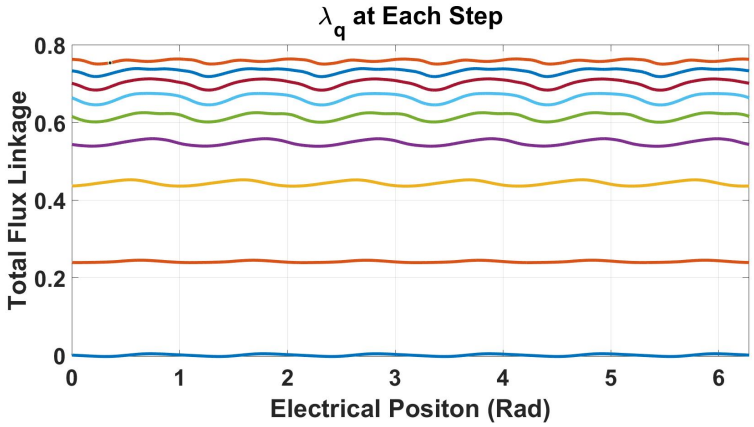

Figure 4.4: λ_q at each step.

2. Extract the data from all steps of injection but at one and the same electrical position, and plot them with i_{dq} as the x-axis and λ_{dq} as the y-axis (2 plots, one for the d axis and the another one is for the q axis). Note that for the q axis, starting from the $i_q = 0$ to i_q at the operating point, but for the d axis, starting from i_d at the operating point to i_d=0. Then, for better accuracy, apply interpolation between each step. The results are the relations between the current and flux linkage in d and q axes at this chosen electrical position, i.e., $\lambda_d(i_d, i_q)\Big|_{\theta_{ef}}$ and $\lambda_q(i_d, i_q)\Big|_{\theta_{ef}}$ which are to be used in (3.30) and (3.31). Note that different paths of injection may give different relations, but ultimately, they all will give the same stored field energy and torque. For the example, this step is illustrated in Fig. 4.5 and 4.6.

3. Apply integral with respect to the current to the relations obtained from step 2. Note that the integration here is the area under the curve and its sign is assigned to be positive. The results of the integrations will be the d and q axis current co-energy at the chosen electrical position, i.e., $\widetilde{W}^c_{i_{df},\theta_{ef}}$ and $\widetilde{W}^c_{i_{qf},\theta_{ef}}$ of (3.30) and (3.31). Fig.4.7 and 4.8 illustrate this process according to the example.

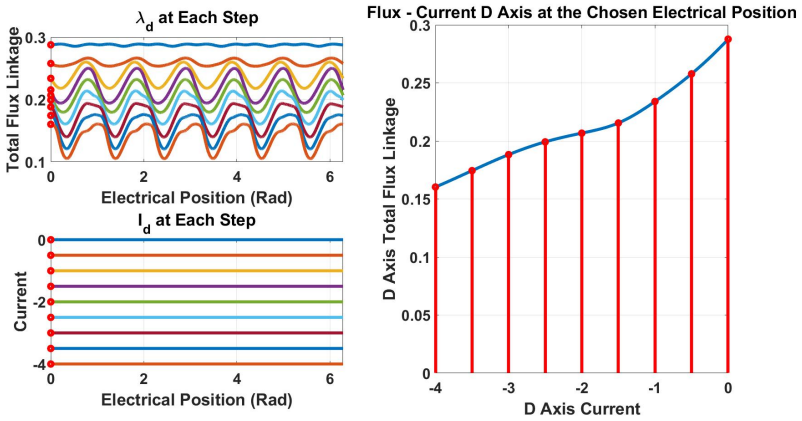

Figure 4.5: Relation between λ_d and i_d at a specific electrical position in the example.

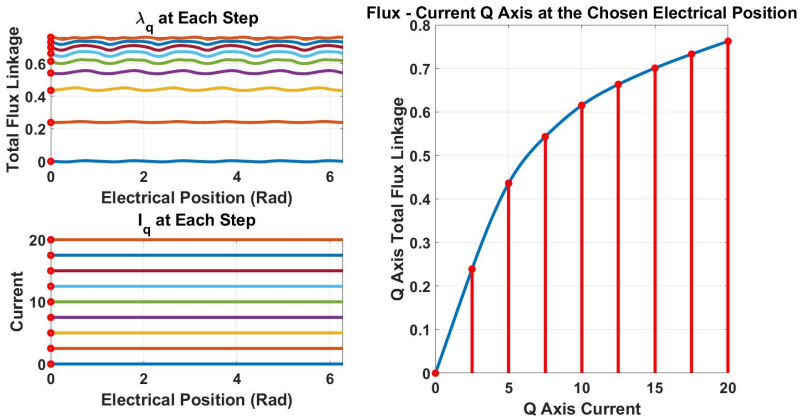

Figure 4.6: Relation between λ_q and i_q at a specific electrical position in the example.

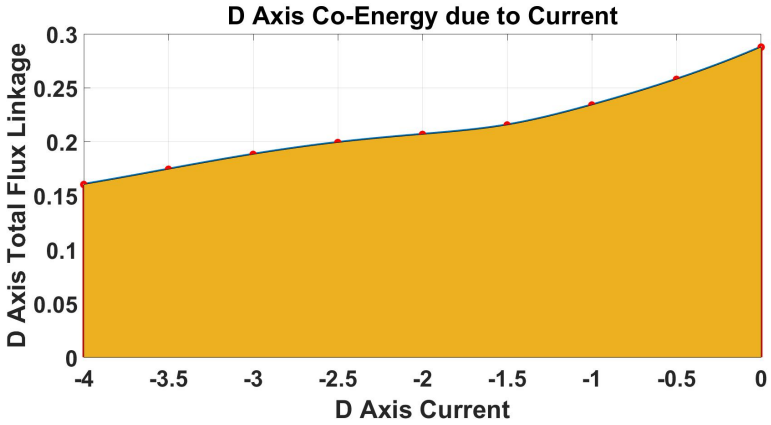

Figure 4.7: Integration in d Axis.

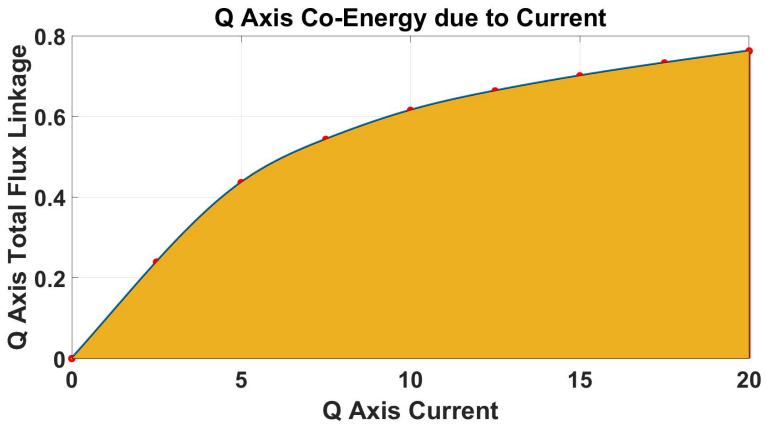

Figure 4.8: Integration in q Axis.

4. Repeat steps 2 and 3 for every electrical position of the collected data. Then, by stacking the resulting current co-energy at all electrical positions together, the complete current co-energy functions over an entire range of electrical positions in the d and q axis, $\widetilde{W}^c_{i_{df}}(\theta_e)$ and $\widetilde{W}^c_{i_{qf}}(\theta_e)$, can be obtained. In the example, the complete current co-energy functions are shown in Fig. 4.9 and 4.10.

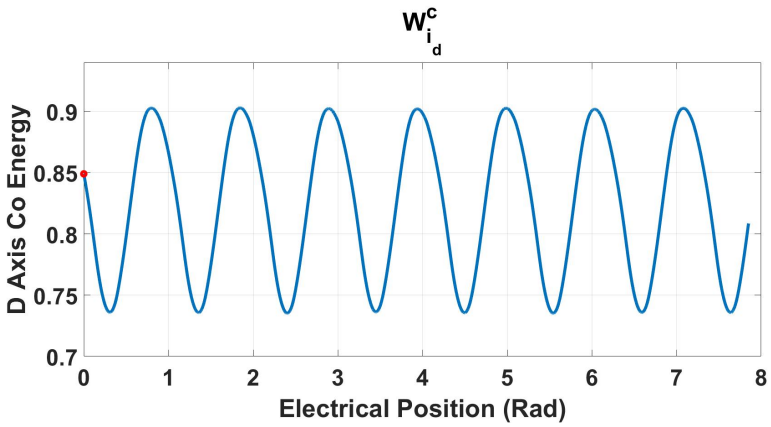

Figure 4.9: Co-energy function in d Axis.

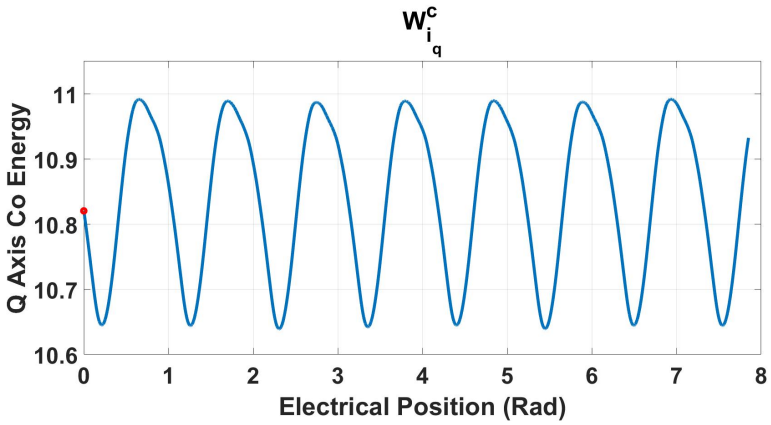

Figure 4.10: Co-energy function in q Axis.

5. The final step is to substitute all terms into (3.29). The terms $\widetilde{W}^c_{i_{df},\theta_{ef}}$ and $\widetilde{W}^c_{i_{qf},\theta_{ef}}$ are obtained from the previous step. The terms λ_{dqf} and i_{dqf} are from the collected data at the step of the operating point. As for the cogging torque, it is assumed to be known. In the example, the stored field energy torque is shown in Fig. 4.11.

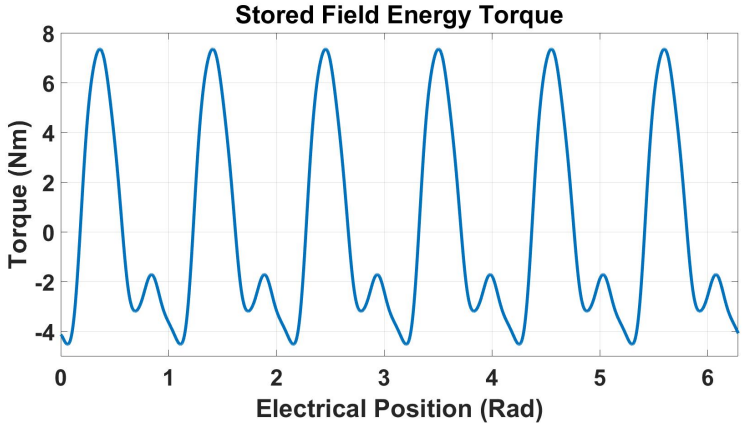

Figure 4.11: Stored field energy torque at the operating point.

4.2 Instantaneous Torque

Calculation of the instantaneous torque is comparatively easier than that of the stored field energy torque. It can be done simply by applying (3.9) directly at the operating point. The important thing here is that all harmonics must be included. Fig. 4.12 shows λ_{dq} at the operating point and Fig. 4.13 shows the corresponding instantaneous torque.

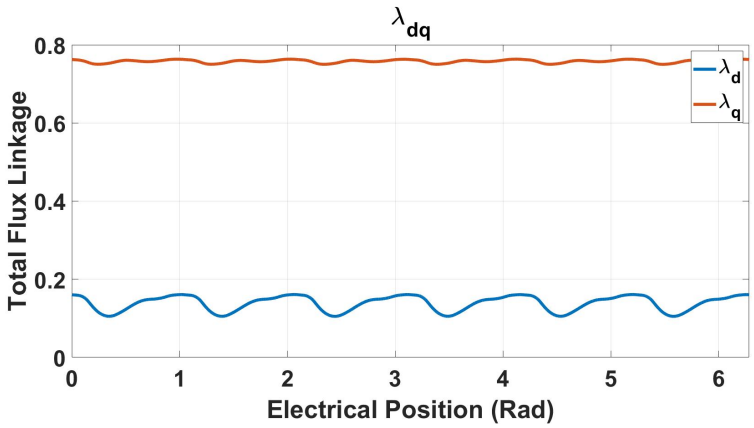

Figure 4.12: λ_{dq} at the operating point.

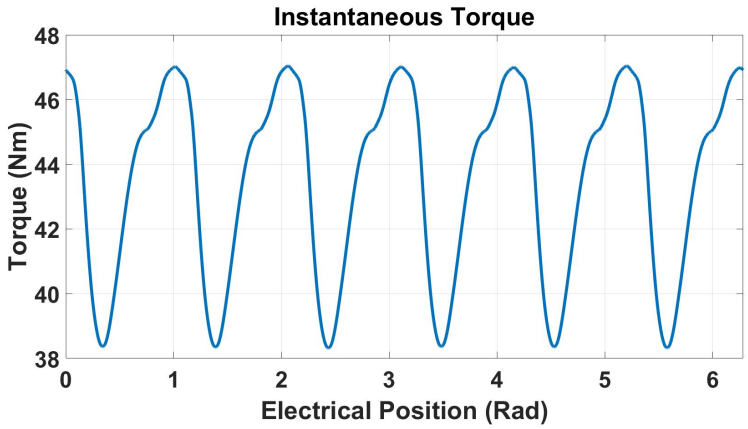

Figure 4.13: Instantaneous torque at the operating point.

4.3 Total Torque

Finally, adding the two torques gives the total torque of IPMSMs (3.32). In the example, the torque calculated by FEA and the torque from the estimation are compared in Fig. 4.14.

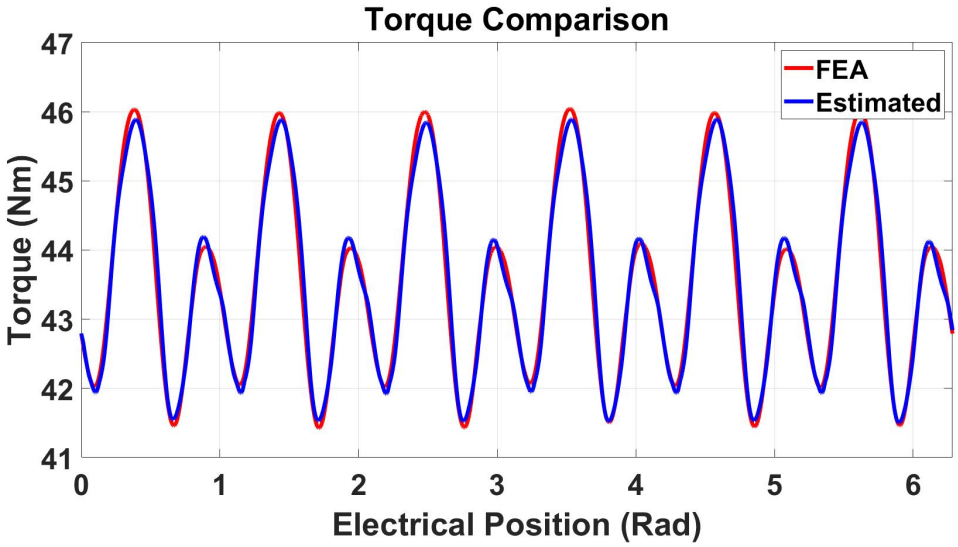

Figure 4.14: Comparison between the torque calculated by FEA and the estimated torque using the algorithm.

One of the most important things is that by considering each step of injection as another operating point and repeating the calculation presented above, the torque at any point on the path of injection can be obtained. For example, suppose the path of injection is chosen to be the curve line in Fig. 4.2, after injecting the current step by step to the operating point (i_{dop}, i_{qop}), the ultimate result is the torque at any point over the entire curve.

Chapter 5

Torque Pulsation Reduction of IPMSMs

For a given desired level of torque, the idea in torque pulsation reduction by means of control is to inject less current when the torque is higher than the desired level. On the other hand, when the torque is lower than the desired level, inject more current. By doing so, it is expected that the injected current will compensate the torque, making it constant. In this work, the current is called "reducing torque pulsation current."

For IPMSMs, provided that the torque pulsation is known, the problem is reduced to how to calculate the reducing torque pulsation current. The analytical calculation is not simple. To illustrate the reason, suppose the total torque, (3.32), had only the instantaneous term, it seems that once λ_{dq} are known, the reducing torque pulsation current could be calculated without any difficulties. However, that is definitely not the case. This is because due to the saturation, the waveforms of λ_{dq} depend heavily on the level of current. Once the normal current is replaced by the reducing torque pulsation current, the waveforms of λ_{dq} will deviate. Since the reducing torque pulsation current was calculated based on the first waveforms of λ_{dq}, this current would not reduce the torque pulsation as much as it should. Moreover, if the stored field energy torque is taken back into consideration, the complexity will become much higher.

One possible analytical solution is to first identify the relation between the level of current, total flux linkage and the co-energy and then calculate the reducing torque pulsation current accordingly. However, this is equivalent to creating a look-up table.

Hence, it would be much simpler to create a look-up table for the torque directly, instead of this relation. The idea in using a look-up table to reduce the torque pulsation is the following. Given a desired operating point, first identify the torque pulsation at neighboring operating points for at least one electrical cycle. This would allow creation of a look-up table with current and electrical position as inputs and torque as an output. Then, by inverting the table at some desired constant torque, the reducing torque pulsation current can be obtained.

The next question is what should be the neighboring operating points mentioned above. The answer depends on which current will be used to reduce the torque pulsation. For IPMSMs, this could be only i_d, only i_q or both. The important thing is that the look-up table can be inverted only when the desired constant torque is below the minimum of the torque from the highest current and above the maximum of the torque from the lowest current in the table.

For example, suppose that some IPMSM is desired to be operated at $i_d = -13.7A$ and $i_q = 100A$. The task is to reduce the torque pulsation by using only i_q. The neighboring operating points are chosen at $i_q = 80, 120$ and $140A$ while i_d is kept fixed at $-13.7A$. The corresponding torque of each level, including that of the desired operating point, are shown in Fig. 5.1. Note that these torques will be used to create the look-up table and its acceptable range is between the two black lines.

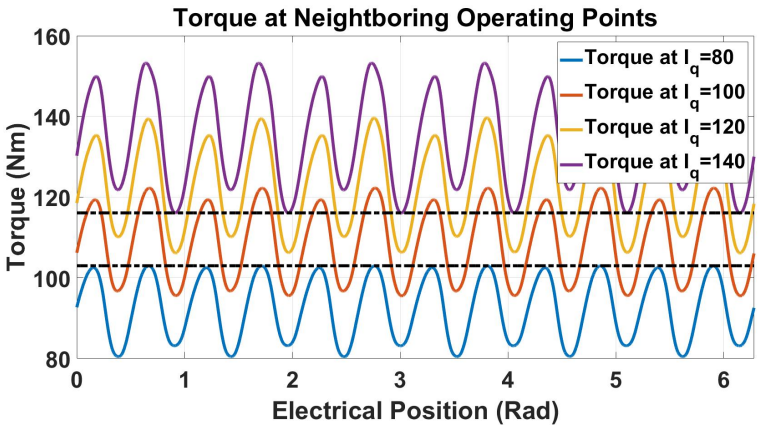

Figure 5.1: Torque at neighboring operating points.

Suppose that the desired operating point has the average torque of 108Nm. By inverting the table at 108Nm, the reducing torque pulsation current can then be obtained, as shown in Fig 5.2.

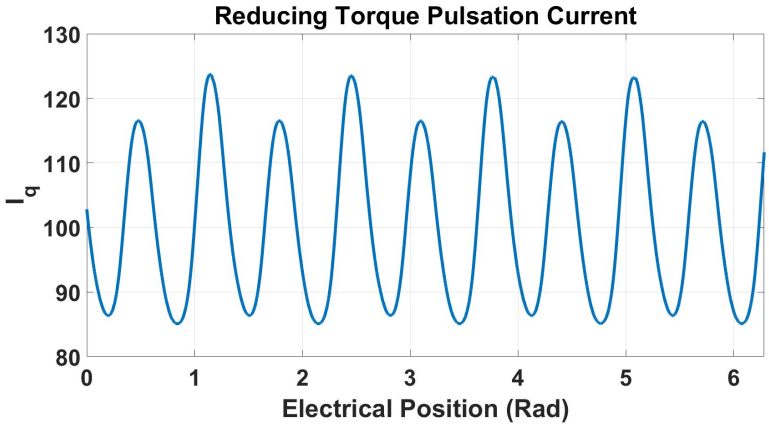

Figure 5.2: Reducing torque pulsation current at 108Nm obtained by inverting the table.

Chapter 6

Total Flux Linkage Estimation

In the torque estimation algorithm, the waveforms of the total flux linkage in d and q axis are needed. They can be obtained by integrating the phase back-emfs and transforming them to d-q quantities as (6.1).

$$\lambda_{dq} = T_{abc \to dq}\Big[\int \big(v_{abc} - i_{abc} r_s\big) dt\Big] \tag{6.1}$$

where r_s is the resistance of the stator winding, v_{abc} is the phase terminal voltages and $T_{abc \to dq}$ is the transformation matrix.

However, the phase terminal voltages v_{abc} are usually inaccessible since most of the time, the motor is driven by PWM. Due to this reason, v_{abc} are replaced by the reference voltages of the PWM $\hat{v}_{abc}$.

Chapter 7

Simulation Results

The motor used in this chapter is the same motor used in the examples previously. For convenience, its specification is repeated here. The motor is a 10-pole IPMSM with concentrated windings and fractional slot per pole per phase. The rated current is $I_s = 25A$ and its MTPA is approximately at 110°, for all I_s. Its cogging torque is shown in Fig 7.1.

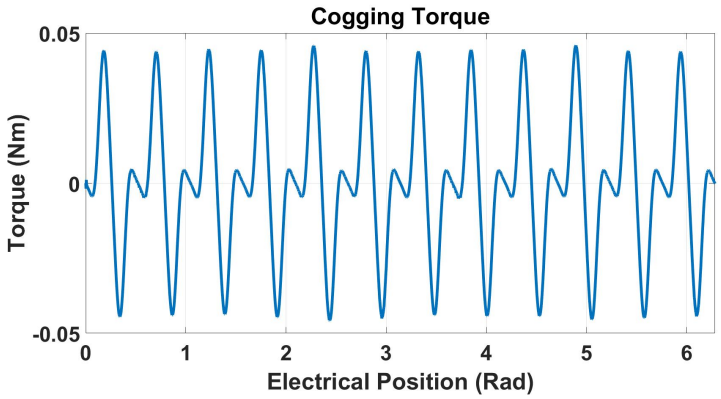

Figure 7.1: Cogging Torque.

7.1 Torque Pulsation Estimation — Constant I_{dq}

To illustrate the accuracy of the proposed estimation method among the other methods in literature, three important methods are chosen from the literature, and their estimates are compared to the estimate from the proposed method and the torque from FEA. The comparison will be made at $I_s = 2, 12$ and $22A$, all at 110°, which represent no, moderate and heavy magnetic saturations.

The path of injection in the proposed method is $I_s = 2A - 22A$ with a step size of $2A$, all at 110°, and the three methods are based on the following equations (7.1), (7.2) and (7.3).

$$T = \frac{3}{2}P(\lambda_d i_q - \lambda_q i_d) \tag{7.1}$$

$$T = \frac{\widetilde{e}_a i_a + \widetilde{e}_b i_b + \widetilde{e}_c i_c}{\omega_m} \tag{7.2}$$

$$T = \frac{3}{2}P\left[\frac{1}{2}[i_{dq}]^T \frac{d[\phi_{dq}]}{d\theta_e} - \frac{1}{2}[\phi_{dq}]^T \frac{d[i_{dq}]}{d\theta_e} + [i_{dq}]^T \frac{d[\psi_{dq}]}{d\theta_e} + [\lambda_{Fdq}]^T \times [i_{dq}]\right] + T_{cogging} \tag{7.3}$$

where $\widetilde{e}_{abc}$ are no-load phase back-emfs, i_{abc} are phase currents, λ_{dq}, ψ_{dq} and i_{dq} are d-q axis total flux linkages, flux linkages from the magnets and currents respectively. ω_m is the mechanical speed in (rad/s), θ_e is the electrical position in radians, P is the number of pole pairs, $T_{cogging}$ is the cogging torque and all the matrices are defined as below with $[\lambda_{Fdq}]$ is the average value of $[\lambda_{dq}]$ and $[\phi_{dq}] = [\lambda_{dq}] - [\psi_{dq}]$.

$$[\lambda_{dq}] = \begin{bmatrix} \lambda_d \\ \\ \lambda_q \end{bmatrix}$$

$$[\psi_{dq}] = \begin{bmatrix} \psi_d \\ \\ \psi_q \end{bmatrix}$$

$$[i_{dq}] = \begin{bmatrix} i_d \\ \\ i_q \end{bmatrix}$$

Equation (7.1) is the general torque equation for IPMSMs that is normally used in control applications. Equation (7.2) is one of the traditional torque equations for the torque pulsation [2]. Equation (7.3) is one of the recent and promising analytical torque equations of IPMSMs that, similar to this work, was derived based on the concept of co-energy [13].

The comparisons are shown in Fig. 7.2, 7.3 and 7.4. In each figure, the red plot is the torque obtained from FEA. The pink, black and green plots are the torque obtained by using (7.1), (7.2) and (7.3) respectively, and the blue plot is the torque obtained by using the proposed estimation method.

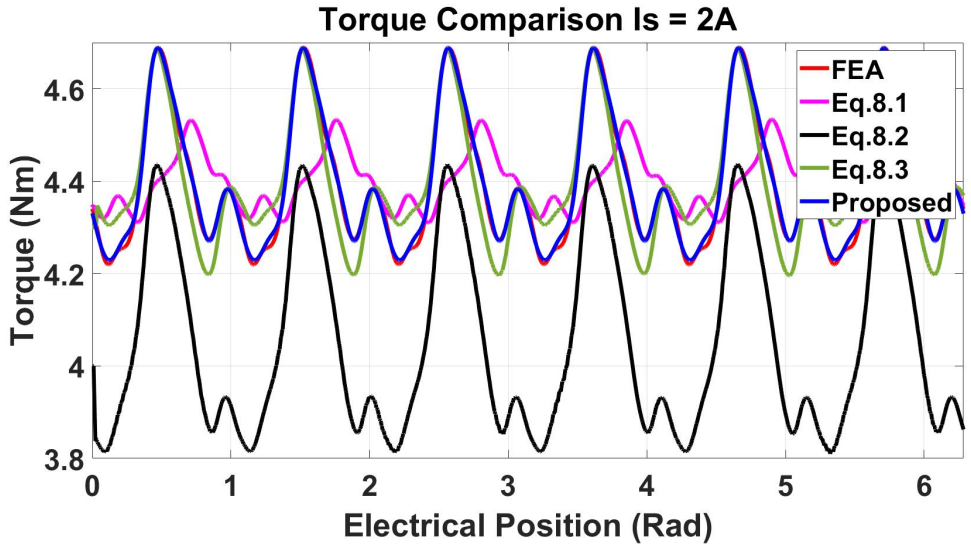

Figure 7.2: Comparison of torque estimations based on eq. 7.1, 7.2 and 7.3 at $I_s = 2A$.

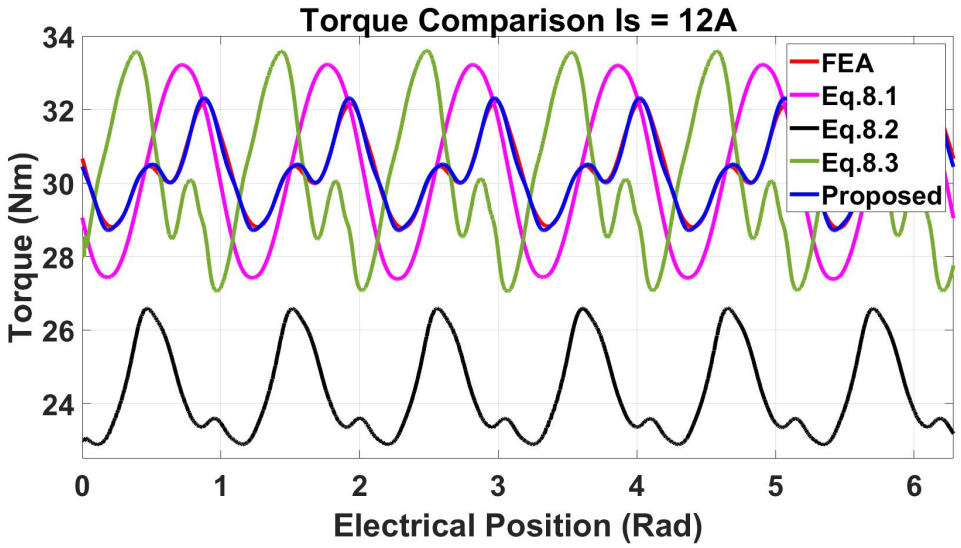

Figure 7.3: Comparison of torque estimations based on eq. 7.1, 7.2 and 7.3 at $I_s = 12A$.

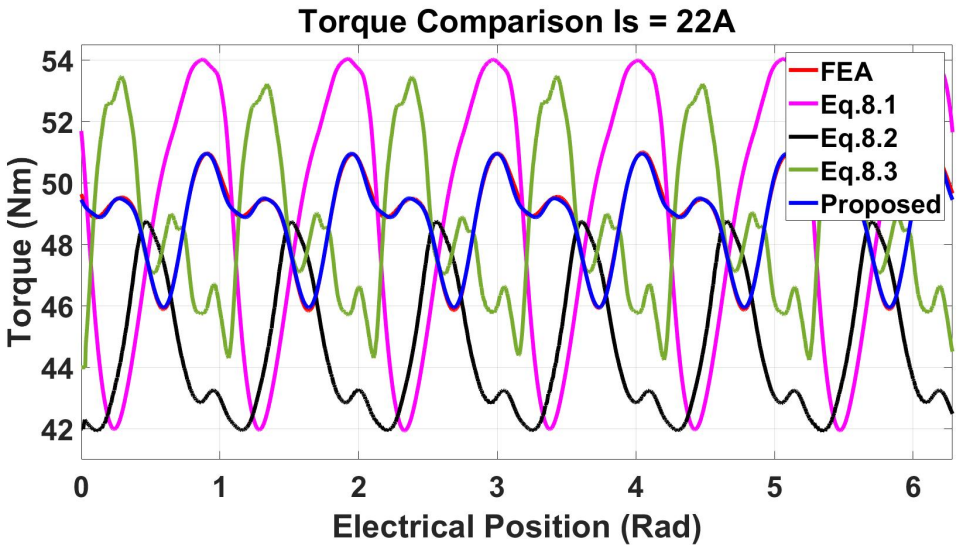

Figure 7.4: Comparison of torque estimations based on eq. 7.1, 7.2 and 7.3 at $I_s = 22A$.

It can be seen that (7.2) completely fails to estimate the torque in all cases. Equation (7.1) can estimate the average torque correctly in all cases but fails to estimate the pulsation. This is because the equation considers only the instantaneous torque. Equation (7.3) can estimate the average torque correctly but can estimate the pulsation only at $I_s = 2A$, where there is no magnetic saturation. The reason is that the co-energy used in the derivation of the equation was not thoroughly defined and the structure of the equation itself was based on linear magnetic saturation. As for the proposed method, it can estimate the torque accurately in all cases.

To further express that the proposed estimation method is valid and accurate for any operating point, the path of injection is extended to $I_s = 26A$, with a step size of $2A$, all at $110°$, and the estimation method is then applied to each step. Fig. 7.5, 7.6 and 7.7 show comparisons of the torques at all steps between those obtained by FEA (Red) and those obtained by using the proposed estimation method (Blue). It can be seen that the method can estimate the torque pulsation very accurately and for any operating point.

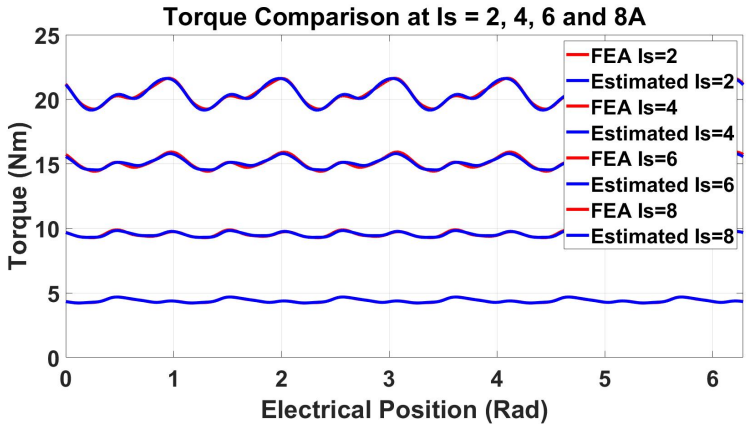

Figure 7.5: Torque comparison at $I_s = 2, 4, 6$ and $8A$.

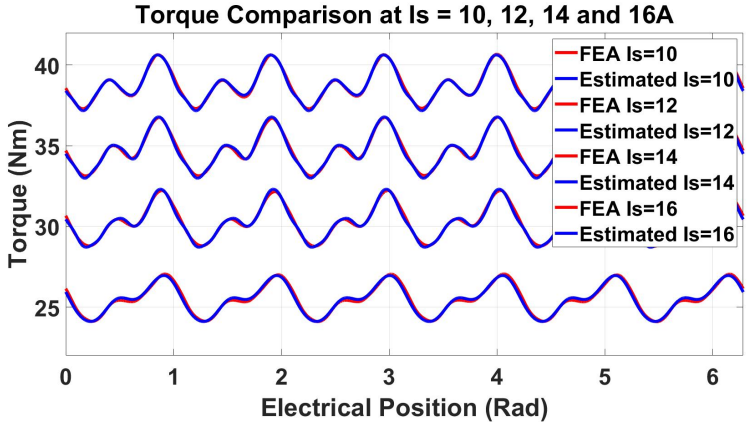

Figure 7.6: Torque comparison at $I_s = 10, 12, 14$ and $16A$.

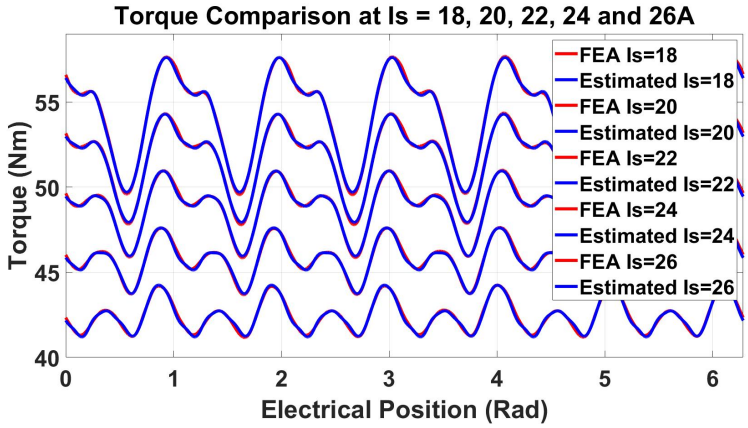

Figure 7.7: Torque comparison at $I_s = 18, 20, 22, 24$ and $26A$.

7.2 Torque Pulsation Estimation — Oscillating I_{dq}

To show that the estimation does not require i_{dq} to be constant, this section repeats the previous section but with $0.5sin(6\omega_s t)$ and $0.5cos(6\omega_s t)$ added into i_d and i_q respectively at each step of injection. The waveforms of the i_{dq} and their corresponding λ_{dq} at each step of injection are shown in Fig. 7.8 to 7.11, and the comparisons of the torques are shown in Fig. 7.12, 7.13 and 7.14.

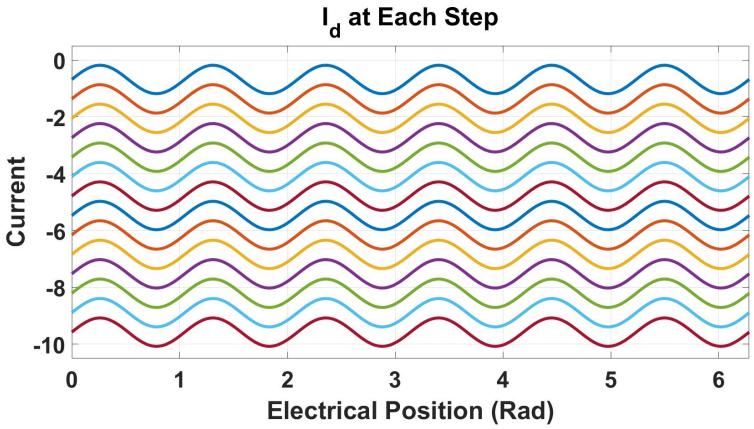

Figure 7.8: i_d at each step.

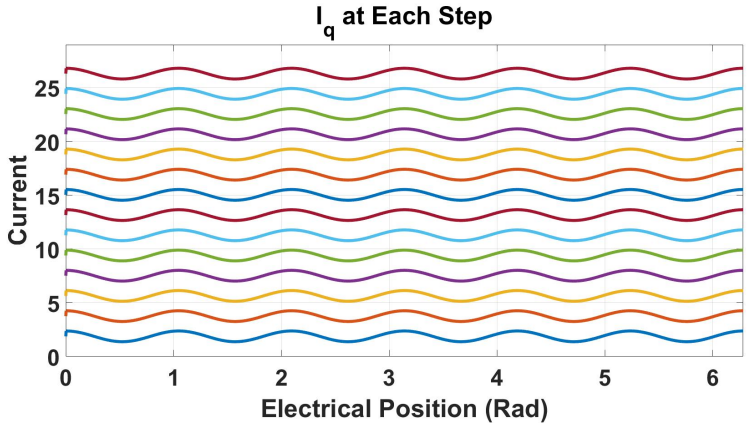

Figure 7.9: i_q at each step.

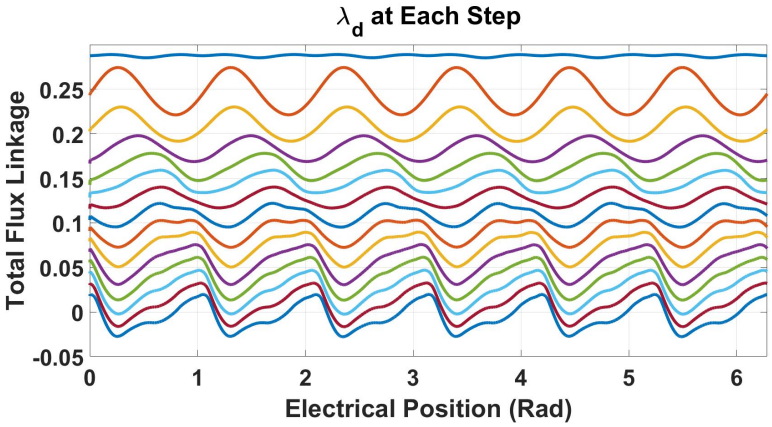

Figure 7.10: λ_d at each step.

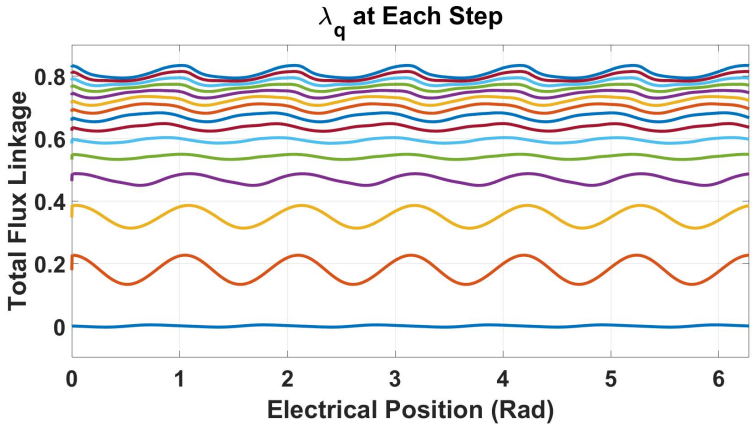

Figure 7.11: λ_q at each step.

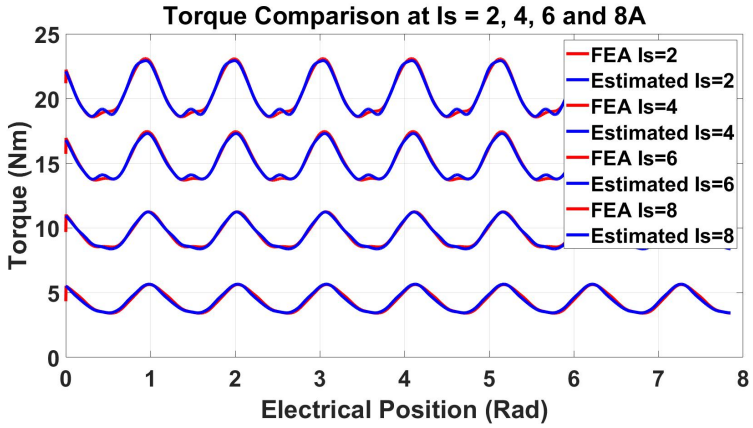

Figure 7.12: Torque comparison at $I_s = 2, 4, 6$ and $8A$.

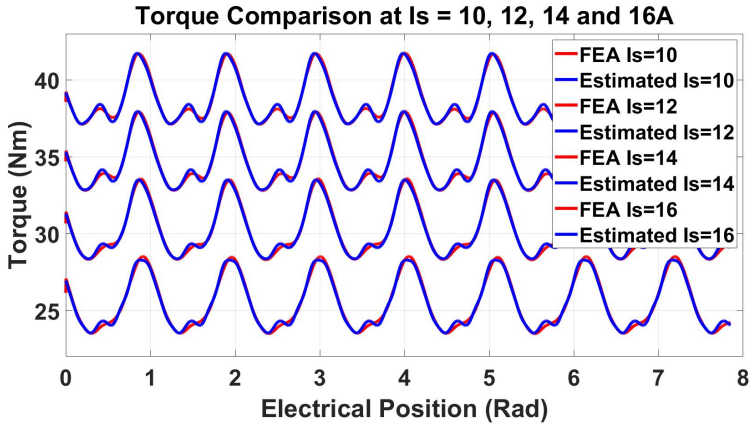

Figure 7.13: Torque comparison at $I_s = 10, 12, 14$ and $16A$.

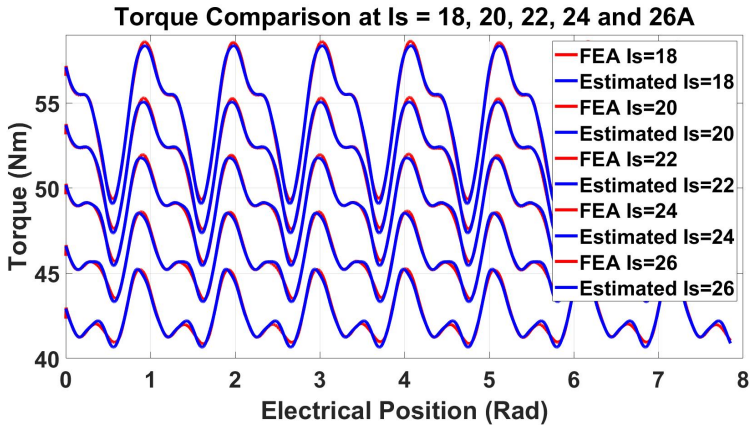

Figure 7.14: Torque comparison at $I_s = 18, 20, 22, 24$ and $26A$.

In order to verify the fact that the estimation algorithm is accurate and valid for any current waveform, arbitrary waveforms of current are injected into the motor. Then, the estimation method is applied. The arbitrary waveforms of current are shown in Fig. 7.15 and 7.16 and the comparison of the torques is shown in Fig. 7.17.

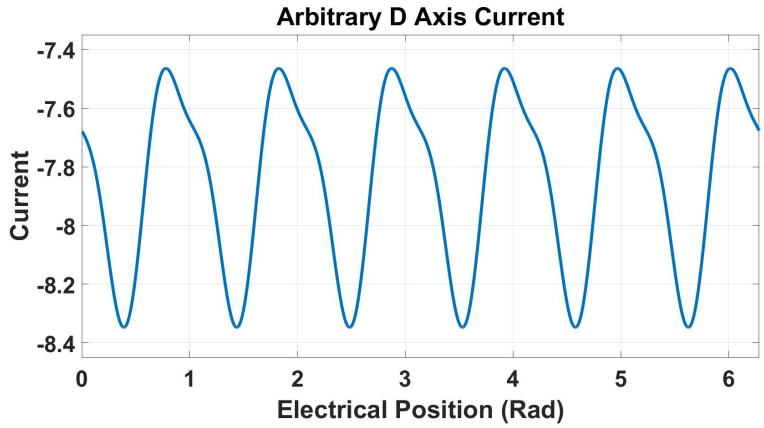

Figure 7.15: Arbitrary i_d.

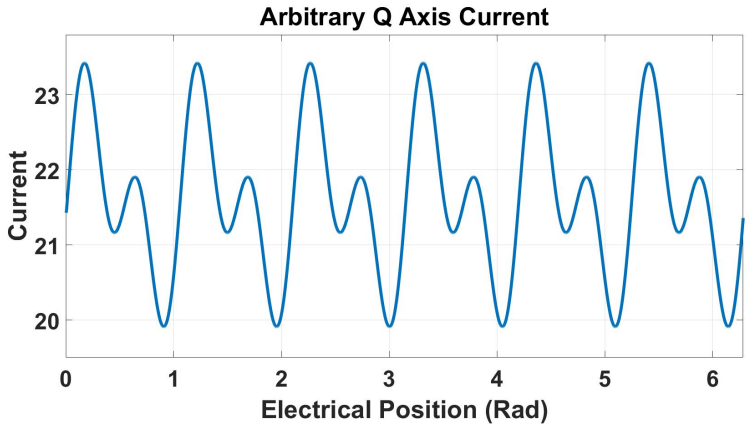

Figure 7.16: Arbitrary i_q.

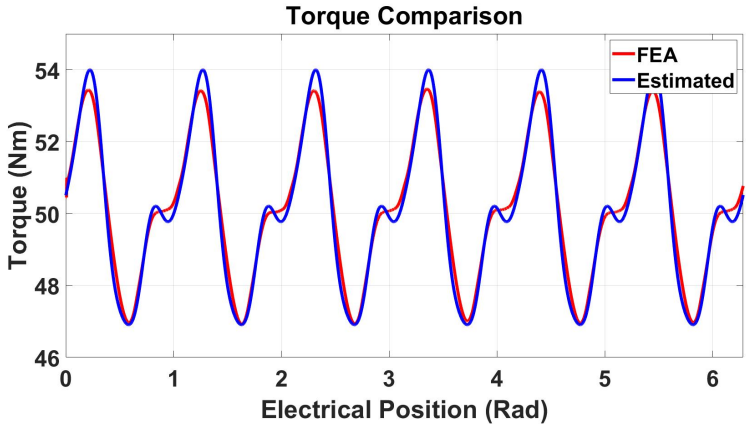

Figure 7.17: Torque comparison under arbitrary current waveforms.

7.3 Torque Pulsation Reduction

By using the estimated torques of $I_s = 2A$ to $I_s = 26A$, the look-up table is created. It is assumed here that the task is to reduce the torque pulsation at $I_s = 22A$. By inverting the table at the torque value of this point, the reducing torque pulsation currents, in both d and q axes, can be obtained and are shown in Fig. 7.18 and 7.19. The comparison of the torque without and with the torque pulsation reduction is shown in Fig. 7.20.

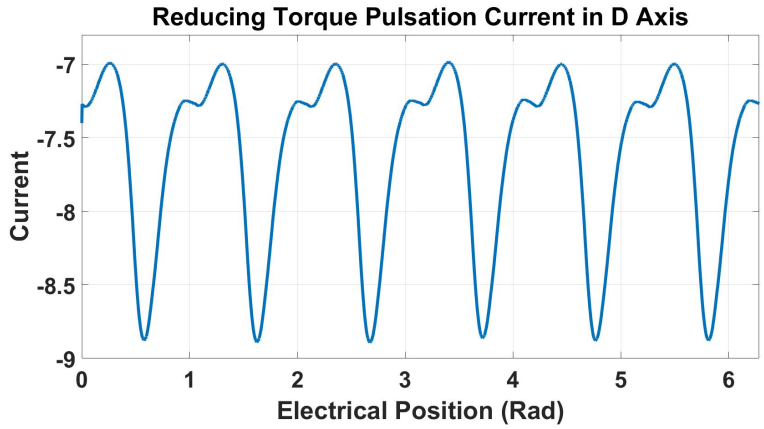

Figure 7.18: Reducing torque pulsation current in d axis.

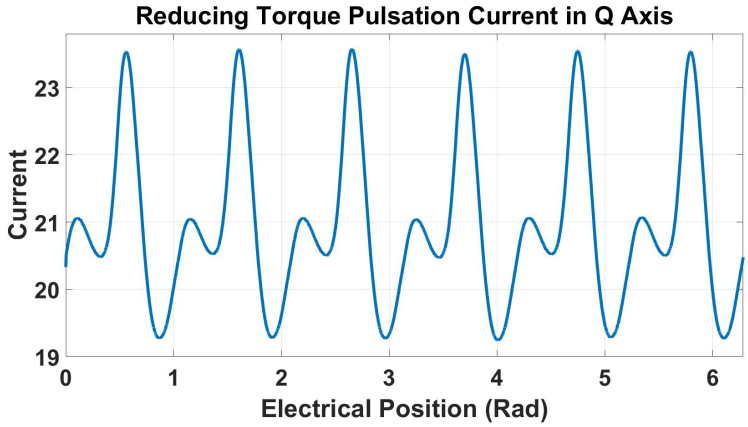

Figure 7.19: Reducing torque pulsation current in q axis.

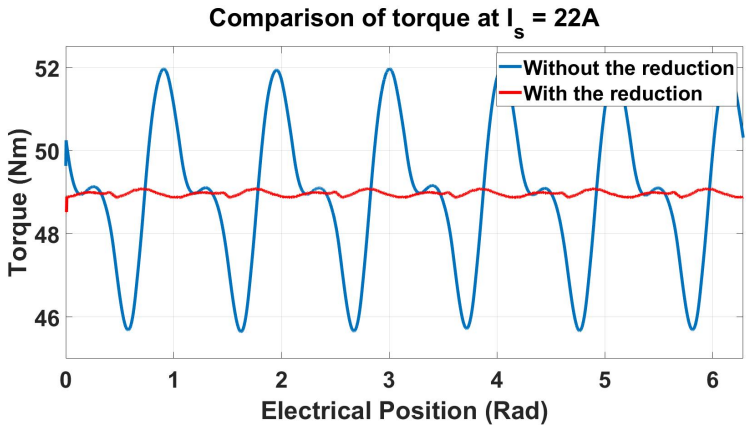

Figure 7.20: Torque without and with the torque pulsation reduction at $I_s = 22A$.

Chapter 8

Experimental Results

The motor used in this experiment is the motor of the 2-D cross section that has been used throughout this work. The setup is shown in Fig. 8.1. In the figure, the dark blue motor is the test motor. It is connected to a dynamometer (light blue motor) which helps maintaining constant rotor speed. The test motor is also connected to a torque transducer. Note that the torque obtained from this transducer is used only for comparison. As for the cogging torque, it is obtained from FEA simulation.

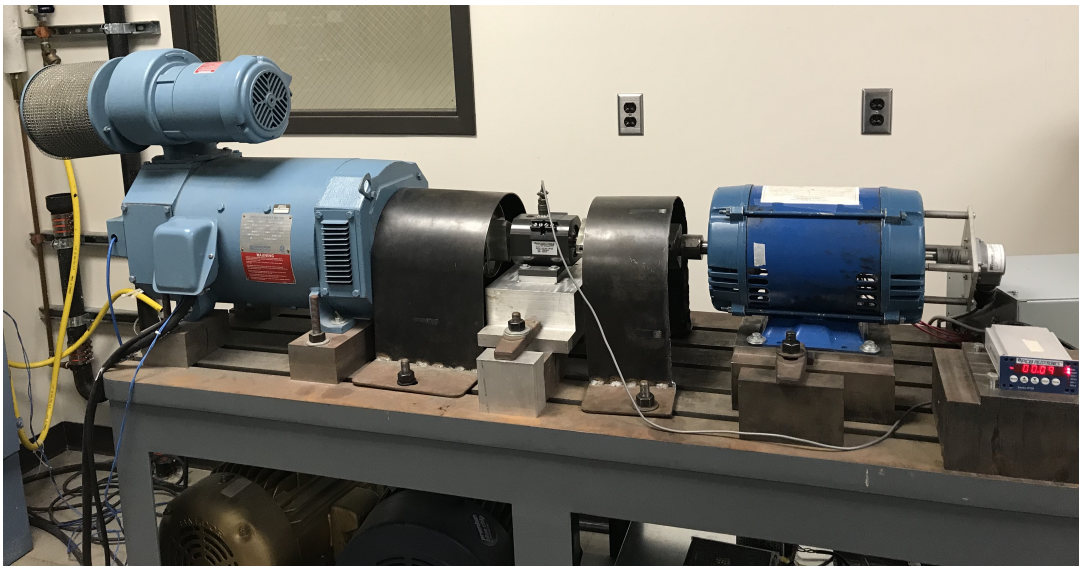

Figure 8.1: Experiment Setup.

The desired operating point in this experiment is assumed to be $I_s = 22.5A$ with 110° and the task here is to reduce the torque pulsation at this point. The path of injection is chosen to be from $I_s = 2A$ to $30A$ with a step size of $2A$, all at 110°.

Fig. 8.2-8.5 show the comparisons of the torque obtained from the transducer (Red) and the torque obtained by the estimation (Blue) of $I_s = 18, 20, 22$ and $24A$ at $110°$.

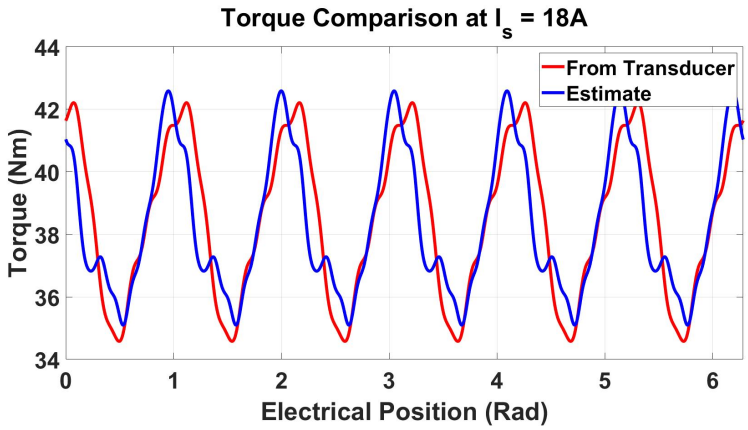

Figure 8.2: $I_s = 18A$.

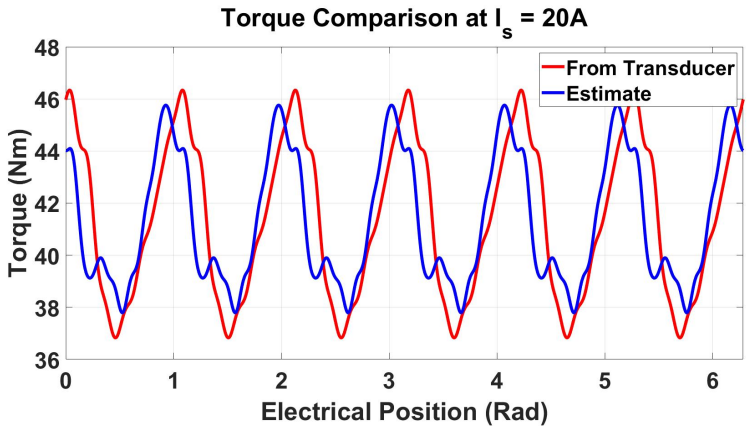

Figure 8.3: $I_s = 20A$.

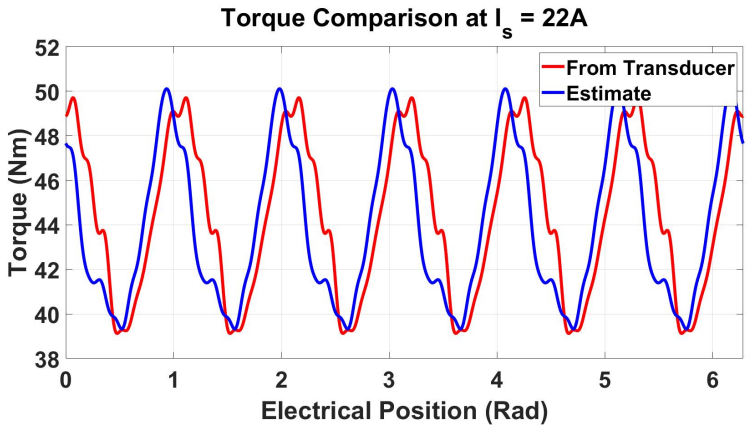

Figure 8.4: $I_s = 22A$.

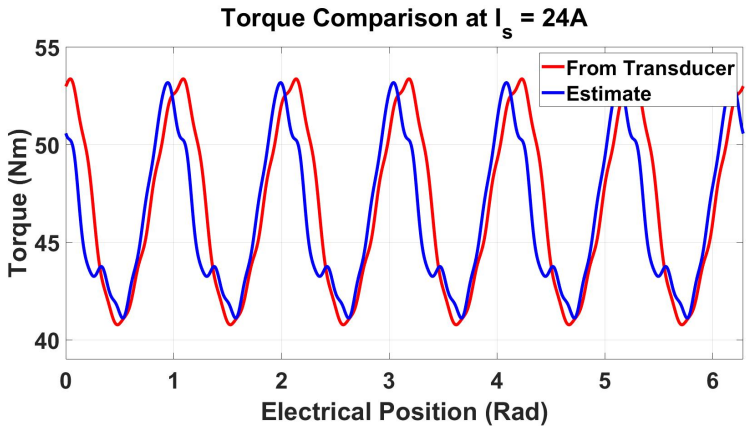

Figure 8.5: $I_s = 24A$.

Using the estimated torques from each step of injection, the look-up table is created. Then, by inverting the table at the torque level of $I_s = 22.5A$ at 110°, the reducing torque pulsation current in d and q axis can be obtained. They are shown in Fig. 8.6 to 8.7. The comparison of the torque without and with the torque pulsation reduction by injecting these currents is shown in Fig. 8.8.

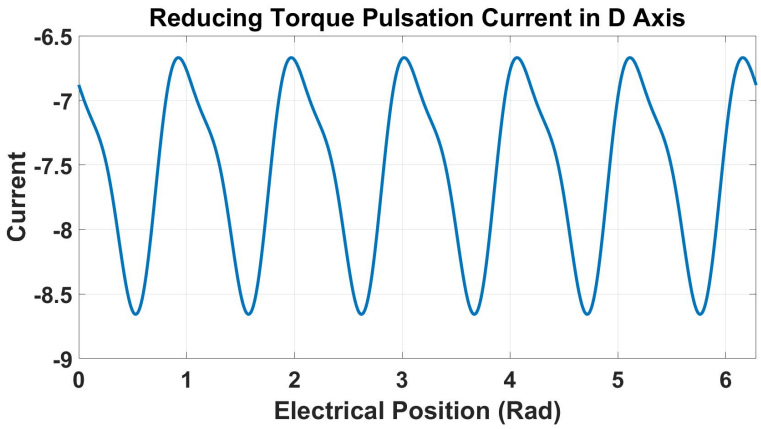

Figure 8.6: Reducing torque pulsation current in d axis.

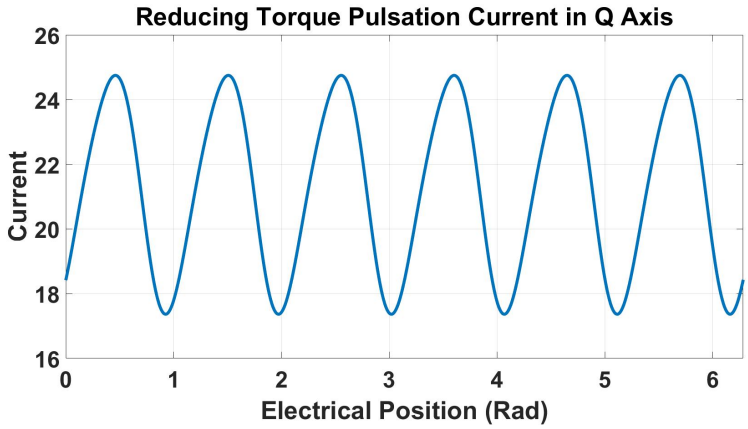

Figure 8.7: Reducing torque pulsation current in q axis.

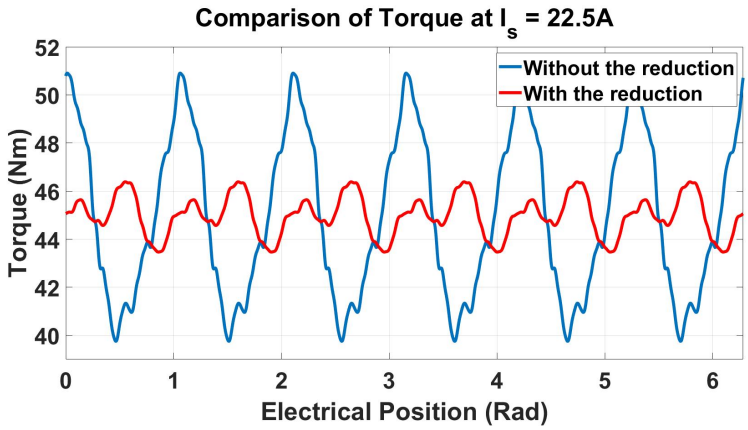

Figure 8.8: Torque without and with the torque pulsation reduction from the transducer at $I_s = 22.5A$.

Chapter 9

Conclusion and Possible Future Work

In this work, a novel method in torque pulsation estimation and reduction of IPMSMs are proposed. This work significantly differs from other similar works in literature in the fact that the proposed estimation method is valid and accurate for any operating point, including that under heavy magnetic saturation region, and for any current waveform. Simulation and experimental results show that the proposed method is valid, accurate and effective.

Nevertheless, the proposed estimation method has two requirements. First, it requires the cogging torque to be known in advanced. In the case that the cogging torque is not known, the torque pulsation can still be estimated and reduced. However, this torque pulsation is the total torque pulsation with the subtraction of the cogging torque, not the total one. Second, it requires a motor to be connected to a dynamometer or a variable mechanical load. However, by doing so only one time, not only can the torque at a specific operating point be estimated, but the torque at any point within the path of injection can also be estimated.

One possible future work is to have the method online. It is expected that by doing so, the accuracy of the method may decrease. In this case, the problem may lie in how to maintain the accuracy within a given acceptable level. Other possible future works may include cogging torque estimation of IPMSMs and analysis of influence of the eddy and hysteresis loss on the estimation method.

BIBLIOGRAPHY

BIBLIOGRAPHY

[1] T. M. Jahns and W. L. Soong, "Pulsating torque minimization techniques for permanent magnet AC motor drives-a review," in IEEE Transactions on Industrial Electronics, vol. 43, no. 2, pp. 321-330, April 1996.

[2] H. Le-Huy, R. Perret and R. Feuillet, "Minimization of Torque Ripple in Brushless DC Motor Drives," in IEEE Transactions on Industry Applications, vol. IA-22, no. 4, pp. 748-755, July 1986.

[3] E. Favre, L. Cardoletti and M. Jufer, "Permanent-magnet synchronous motors: a comprehensive approach to cogging torque suppression," in IEEE Transactions on Industry Applications, vol. 29, no. 6, pp. 1141-1149, Nov.-Dec. 1993.

[4] D. C. Hanselman, "Minimum torque ripple, maximum efficiency excitation of brushless permanent magnet motors," in IEEE Transactions on Industrial Electronics, vol. 41, no. 3, pp. 292-300, June 1994.

[5] P. Mattavelli, L. Tubiana and M. Zigliotto, "Torque-ripple reduction in PM synchronous motor drives using repetitive current control," in IEEE Transactions on Power Electronics, vol. 20, no. 6, pp. 1423-1431, Nov. 2005.

[6] K. Y. Cho, J. D. Bae, S. K. Chung and M. J. Youn, "Torque harmonics minimization in PM synchronous motor with back EMF estimation," Proceedings of TENCON '93. IEEE Region 10 International Conference on Computers, Communications and Automation, Beijing, China, 1993, pp. 589-593 vol.5.

[7] G. Lee, S. Kim, J. Hong and J. Bahn, "Torque Ripple Reduction of Interior Permanent Magnet Synchronous Motor Using Harmonic Injected Current," in IEEE Transactions on Magnetics, vol. 44, no. 6, pp. 1582-1585, June 2008.

[8] L. Guo and L. Parsa, "Torque ripple reduction of the modular Interior Permanent Magnet machines using optimum current profiling technique," 2009 IEEE International Electric Machines and Drives Conference, Miami, FL, 2009, pp. 1094-1099.

[9] Se-Kyo Chung, Hyun-Soo Kim, Chang-Gyun Kim and Myung-Joong Youn, "A new instantaneous torque control of PM synchronous motor for high-performance direct-drive applications," in IEEE Transactions on Power Electronics, vol. 13, no. 3, pp. 388-400, May 1998

[10] N. Y. A. Qamar and C. J. Hatziadoniu, "Cancelation of Torque Ripples in PMSM via a Novel Minimal Parameter Harmonic Flux Estimator," in IEEE Transactions on Power Electronics, vol. 34, no. 3, pp. 2553-2562, March 2019.

[11] M. Barcaro, N. Bianchi and F. Magnussen, "Remarks on Torque Estimation Accuracy in Fractional-Slot Permanent-Magnet Motors," in IEEE Transactions on Industrial Electronics, vol. 59, no. 6, pp. 2565-2572, June 2012.

[12] I. Jeong and K. Nam, "Analytic expression of torque ripple by fourier coefficients of flux linkages," 2015 IEEE International Electric Machines and Drives Conference (IEMDC), Coeur d'Alene, ID, 2015, pp. 127-132.

[13] N. Nakao and K. Akatsu, "Suppressing Pulsating Torques: Torque Ripple Control for Synchronous Motors," in IEEE Industry Applications Magazine, vol. 20, no. 6, pp. 33-44, Nov.-Dec. 2014.

[14] C. Lai, G. Feng, K. L. V. Iyer, K. Mukherjee and N. C. Kar, "Genetic Algorithm-Based Current Optimization for Torque Ripple Reduction of Interior PMSMs," in IEEE Transactions on Industry Applications, vol. 53, no. 5, pp. 4493-4503, Sept.-Oct. 2017.

[15] C. Lai, G. Feng, K. Mukherjee, V. Loukanov and N. C. Kar, "Torque Ripple Modeling and Minimization for Interior PMSM Considering Magnetic Saturation," in IEEE Transactions on Power Electronics, vol. 33, no. 3, pp. 2417-2429, March 2018.

[16] H. Dhulipati, S. Mukundan, C. Lai, K. Mukherjee, J. Tjong and N. C. Kar, "Multiple Reference Frame-Based Extended Concentrated Wound PMSM Model Considering PM Flux Linkage and Inductance Harmonics," in IEEE Transactions on Energy Conversion, vol. 34, no. 2, pp. 731-740, June 2019.

[17] H. Akatsuka and M. Hasegawa, "Torque Ripple Reduction of IPMSM with Concentrated Winding Based on Adaptive Identification of Equivalent Torque Coefficient," 2018 XIII International Conference on Electrical Machines (ICEM), Alexandroupoli, 2018, pp. 1711-1716.

[18] P. L. Chapman, S. D. Sudhoff and C. A. Whitcomb, "Optimal current control strategies for surface-mounted permanent-magnet synchronous machine drives," in IEEE Transactions on Energy Conversion, vol. 14, no. 4, pp. 1043-1050, Dec. 1999.

[19] J.L. Kirtley Jr. 6.061 Introduction to Power Systems Class Notes Chapter 8 Electromagnetic Forces and Loss Mechanisms Massachusetts Institute of Technology: MIT OpenCouseWare, https://ocw.mit.edu/. License: Creative Commons BY-NC-SA.

[20] P.C. Krause, O. Wasynczuk, S.D. Sudhoff, Analysis of Electric Machinery and Drive Systems, 2nd Edition, IEEE Press/Wiley-Interscience, 2003.